

| | | | | | |
|---|-------------------|--------------------------------|--|--|---|
| REPORT DOCUMENTATION PAGE | | | Form Approved OMB NO. 0704-0188 | | |
| <p>The public reporting burden for this collection of information is estimated to average 1 hour per response, including the time for reviewing instructions, searching existing data sources, gathering and maintaining the data needed, and completing and reviewing the collection of information. Send comments regarding this burden estimate or any other aspect of this collection of information, including suggestions for reducing this burden, to Washington Headquarters Services, Directorate for Information Operations and Reports, 1215 Jefferson Davis Highway, Suite 1204, Arlington VA, 22202-4302. Respondents should be aware that notwithstanding any other provision of law, no person shall be subject to any penalty for failing to comply with a collection of information if it does not display a currently valid OMB control number.</p> <p>PLEASE DO NOT RETURN YOUR FORM TO THE ABOVE ADDRESS.</p> | | | | | |
| 1. REPORT DATE (DD-MM-YYYY) 14-05-2015 | | 2. REPORT TYPE Final Report | | 3. DATES COVERED (From - To) 1-Sep-2011 - 28-Feb-2015 | |
| 4. TITLE AND SUBTITLE Final Report: ARO - Terrestrial Research Program, Methodologies and Protocols for Characterization of Geomaterials | | | 5a. CONTRACT NUMBER W911NF-11-1-0430 | | |
| | | | 5b. GRANT NUMBER | | |
| | | | 5c. PROGRAM ELEMENT NUMBER 611102 | | |
| 6. AUTHORS Richard R. Hark, Tom L. Fisher, Russell S. Harmon, Peter A. Defnet, Michael Wise | | | 5d. PROJECT NUMBER | | |
| | | | 5e. TASK NUMBER | | |
| | | | 5f. WORK UNIT NUMBER | | |
| 7. PERFORMING ORGANIZATION NAMES AND ADDRESSES Juniata College 1700 Moore Street Huntingdon, PA 16652 -6124 | | | 8. PERFORMING ORGANIZATION REPORT NUMBER | | |
| 9. SPONSORING/MONITORING AGENCY NAME(S) AND ADDRESS (ES) U.S. Army Research Office P.O. Box 12211 Research Triangle Park, NC 27709-2211 | | | 10. SPONSOR/MONITOR'S ACRONYM(S) ARO | | |
| | | | 11. SPONSOR/MONITOR'S REPORT NUMBER(S) 60674-EV.4 | | |
| 12. DISTRIBUTION AVAILABILITY STATEMENT Approved for Public Release; Distribution Unlimited | | | | | |
| 13. SUPPLEMENTARY NOTES The views, opinions and/or findings contained in this report are those of the author(s) and should not be construed as an official Department of the Army position, policy or decision, unless so designated by other documentation. | | | | | |
| 14. ABSTRACT The third and final year of this project continued to focus on the use of laser-induced breakdown spectroscopy (LIBS) for the analysis of geomaterials. LIBS was utilized for geochemical fingerprinting of an extensive suite carbonate minerals, including those of biogenic origin (sea shells), as well as over 200 garnets obtained from locations around the world. A laboratory-based LIBS instrument was used to produce spectral databases that were subsequently analyzed using chemometric techniques such as partial least-squares discriminant analysis (PLSDA), a common approach for performing statistical regression on high dimensional data. Our results further strengthened | | | | | |
| 15. SUBJECT TERMS laser-induced breakdown spectroscopy, LIBS, chemometrics, partial least squares, discriminant analysis, PLSDA, geochemical fingerprinting | | | | | |
| 16. SECURITY CLASSIFICATION OF: | | | 17. LIMITATION OF ABSTRACT UU | 15. NUMBER OF PAGES | 19a. NAME OF RESPONSIBLE PERSON Tom Fisher |
| a. REPORT UU | b. ABSTRACT UU | c. THIS PAGE UU | | | 19b. TELEPHONE NUMBER 814-641-3563 |

Report Title

Final Report: ARO - Terrestrial Research Program, Methodologies and Protocols for Characterization of Geomaterials

ABSTRACT

The third and final year of this project continued to focus on the use of laser-induced breakdown spectroscopy (LIBS) for the analysis of geomaterials. LIBS was utilized for geochemical fingerprinting of an extensive suite carbonate minerals, including those of biogenic origin (sea shells), as well as over 200 garnets obtained from locations around the world. A laboratory-based LIBS instrument was used to produce spectral databases that were subsequently analyzed using chemometric techniques such as partial least-squares discriminant analysis (PLSDA), a common approach for performing statistical regression on high-dimensional data. Our results further strengthened support for LIBS being an excellent technique for identification and discrimination of minerals based on geographic origin. We successfully explored the use of a stepwise approach for classifying garnets based on first sorting them into one of six classes based on elemental composition followed by PLSDA analysis for provenance determination. We also began a related collaboration with ACE CRREL that focuses on analysis of ice cores for identification of climate change markers. An ongoing goal of our research has been to transition from laboratory-based instruments to the use of handheld LIBS systems for field operations. Though our efforts to obtain funding for such instrumentation did not come to fruition during the time period covered by the grant we now have access to a handheld LIBS unit and plan to repeat many of the same analyses to see if the levels of discrimination are similar. Based on our work over the last several years we did contribute a book chapter dedicated to LIBS-based geochemical fingerprinting.

Enter List of papers submitted or published that acknowledge ARO support from the start of the project to the date of this printing. List the papers, including journal references, in the following categories:

(a) Papers published in peer-reviewed journals (N/A for none)

| <u>Received</u> | <u>Paper</u> |
|-----------------|---|
| 08/30/2013 | 3.00 Russell S. Harmon, Richard E. Russo, Richard R. Hark. Applications of laser-induced breakdown spectroscopy for geochemical and environmental analysis: A comprehensive review, Spectrochimica Acta Part B: Atomic Spectroscopy, (09 2013): 11. doi: 10.1016/j.sab.2013.05.017 |
| 08/31/2012 | 1.00 Chunyi Liu, Richard R. Hark, Jeremiah J. Remus, Lucille J. East, Russell S. Harmon, Michael A. Wise, Benjamin M. Tansi, Katrina M. Shughrue, Kehinde S. Dunsin. Geographical analysis of "conflict minerals" utilizing laser-induced breakdown spectroscopy, Spectrochimica Acta Part B: Atomic Spectroscopy, (06 2012): 131. doi: 10.1016/j.sab.2012.06.052 |
| 08/31/2012 | 2.00 Jeremiah J. Remus, Russell S. Harmon, Richard R. Hark, Gregory Haverstock, Dirk Baron, Ian K. Potter, Samantha K. Bristol, Lucille J. East. Advanced signal processing analysis of laser-induced breakdown spectroscopy data for the discrimination of obsidian sources, Applied Optics, (02 2012): 65. doi: 10.1364/AO.51.000B65 |
| TOTAL: | 3 |

Number of Papers published in peer-reviewed journals:

(b) Papers published in non-peer-reviewed journals (N/A for none)

Received Paper

TOTAL:

Number of Papers published in non peer-reviewed journals:

(c) Presentations

Defnet, P., Hark, R.R., Wise, M., Harmon, R. “Garnet classification and provenance using laser-induced breakdown spectroscopy (LIBS),” CHED 276, Abstract of Papers, 249th American Chemical Society National Meeting, Denver, CO, March 22-26, 2015.

Clausen, J., Bol'shakov, A., Gonzalez, J., Hark, R., Russo, R., Courville, Z., Osterberg, E. “Comparison of LIBS to ICP-MS for analysis of ice,” SciX 2014, Reno, NV, September 28-October 3, 2014.

Clausen, J., Bol'shakov, A., Gonzalez, J., *Hark, R., Russo, R., Courville, Z., “Ice Core Analysis using Laser-Induced Breakdown Spectroscopy (LIBS),” 8th International Conference on Laser Induced Breakdown Spectroscopy (LIBS 2014), Beijing, China, September 8-12, 2014.

Wise, M., Defnet, P.A., *Hark, R.R. Harmon, R.S. “Garnet classification and provenance using laser-induced breakdown spectroscopy (LIBS),” 8th International Conference on Laser Induced Breakdown Spectroscopy (LIBS 2014), Beijing, China, September 8-12, 2014.

Number of Presentations: 4.00

Non Peer-Reviewed Conference Proceeding publications (other than abstracts):

Received Paper

TOTAL:

Number of Non Peer-Reviewed Conference Proceeding publications (other than abstracts):

Peer-Reviewed Conference Proceeding publications (other than abstracts):

Received Paper

TOTAL:

Number of Peer-Reviewed Conference Proceeding publications (other than abstracts):

(d) Manuscripts

Received Paper

TOTAL:

Number of Manuscripts:

Books

Received Book

TOTAL:

TOTAL:

Patents Submitted

Patents Awarded

Awards

None

Graduate Students

| <u>NAME</u> | <u>PERCENT SUPPORTED</u> |
|-----------------|--------------------------|
| FTE Equivalent: | |
| Total Number: | |

Names of Post Doctorates

| <u>NAME</u> | <u>PERCENT SUPPORTED</u> |
|-----------------|--------------------------|
| FTE Equivalent: | |
| Total Number: | |

Names of Faculty Supported

| <u>NAME</u> | <u>PERCENT SUPPORTED</u> | National Academy Member |
|----------------------|--------------------------|-------------------------|
| Richard R. Hark, PhD | 0.25 | |
| FTE Equivalent: | 0.25 | |
| Total Number: | 1 | |

Names of Under Graduate students supported

| <u>NAME</u> | <u>PERCENT SUPPORTED</u> | Discipline |
|-----------------|--------------------------|------------|
| Lauren Steigen | 0.20 | |
| FTE Equivalent: | 0.20 | |
| Total Number: | 1 | |

Student Metrics

This section only applies to graduating undergraduates supported by this agreement in this reporting period

The number of undergraduates funded by this agreement who graduated during this period: 0.00

The number of undergraduates funded by this agreement who graduated during this period with a degree in science, mathematics, engineering, or technology fields:..... 0.00

The number of undergraduates funded by your agreement who graduated during this period and will continue to pursue a graduate or Ph.D. degree in science, mathematics, engineering, or technology fields:..... 0.00

Number of graduating undergraduates who achieved a 3.5 GPA to 4.0 (4.0 max scale):..... 0.00

Number of graduating undergraduates funded by a DoD funded Center of Excellence grant for Education, Research and Engineering:..... 0.00

The number of undergraduates funded by your agreement who graduated during this period and intend to work for the Department of Defense 0.00

The number of undergraduates funded by your agreement who graduated during this period and will receive scholarships or fellowships for further studies in science, mathematics, engineering or technology fields: 0.00

Names of Personnel receiving masters degrees

NAME

Total Number:

Names of personnel receiving PHDs

NAME

Total Number:

Names of other research staff

NAME

PERCENT SUPPORTED

FTE Equivalent:

Total Number:

Sub Contractors (DD882)

Inventions (DD882)

Scientific Progress

Summary of Work for Year Three of the Project

During the last year of the project we focused on analysis of suites of carbonate minerals and garnets, developed some new approaches to chemometric analysis, began a collaboration with a scientist at the Army Corps of Engineers Cold Regions Research and Engineering Laboratory, made several presentations at conferences, and contributed a chapter on geochemical fingerprinting using LIBS for a new Springer-Verlag book. Over the past several years our group has assembled a collection of 142 carbonate minerals, which included marbles, limestones, and seashells. We analyzed these materials and carried our preliminary chemometric analysis to determine how well LIBS could distinguish between samples of the same chemical make-up but different forms (e.g. calcite and aragonite) as well as the same mineral from different locations. The chemometric analysis worked well but additional pre-processing of the data is required to handle the large amount of data we generated.

Garnet is a silicate mineral that conforms to the general compositional formula $A_3B_2(SiO_4)_3$, where the 'A' site is occupied by rather large divalent cations (Ca^{2+} , Mg^{2+} , Fe^{2+} , or Mn^{2+}) and the 'B' site hosts smaller trivalent cations (Al^{3+} , Fe^{3+} , or Cr^{3+}). There are six common species of garnet that comprise two groups on the basis of their ideal end-member chemical compositions. Given the compositional variation, garnet is an ideal geomaterial to further test the limits of LIBS analysis. Previously, Alvey et al. (2010, Appl. Opt. 49, C168) analyzed 157 samples described as garnets from 92 locations worldwide using LIBS. In our study, an expanded suite of over 203 garnets was examined using electron microprobe microanalysis (EPMA) to correctly classify the samples on the basis of their major element composition and then ascertain the efficacy of LIBS for classification and provenance determination. The LIBS spectral data were processed using multivariate statistical pattern recognition methods

(PCA, PLSDA) and the resulting classification models then used to successfully classify unknown garnet samples of a specific compositional type according to their geographic origin. We successfully employed a stepwise approach for classifying garnets based on first sorting them into one of the six classes based on elemental composition followed by PLSDA analysis for provenance determination. Various preprocessing techniques (normalization, spectral outlier removal) were implemented to optimize the LIBS classification results. This is the first study in which EPMA, a tool widely used for geochemical analysis, was compared with LIBS on such a large sample collection. Not surprisingly, EPMA and LIBS both did about the same for garnet type classification (~93% correct classification) but when it came to geographic origin we were able to demonstrate that LIBS offers a good alternative for identification of unknown garnet samples based on their geographic provenance. The findings from the garnet study were presented at LIBS 2014 in Beijing, China, the first international LIBS conference to be held in the East. A paper is being written that summarizes this work and we expect to submit during the summer of 2015. The student who did this work was not paid from the ARO grant but is graduating this spring with 3.5+ GPA and will be starting a PhD program at the university of Washington in the fall of 2015.

In conjunction with CRREL, we also began to evaluate LIBS for its ability to detect paleo-climate proxy indicators (Ca, K, Mg, and Na) in ice. Conventional elemental analysis of ice involves melting, digestion, and analysis using inductively coupled plasma – mass spectrometry (ICP-MS). ICP-MS analysis established elemental concentrations in the ppt to ppb range for the ice. In our study LIBS analysis of the ice-core from Summit Station in Greenland was carried out using a thermoelectric Peltier cooling plate to maintain ice integrity. The bulk ice as well as, for the first time, individual dust particles in the ice were characterized. The LIBS results revealed detection of peaks for C and CN, consistent with the presence of organic material, as well as major ions (Ca, K, Mg, and Na) and trace metals (Al, Cu, Fe, Mn, Ti, Zn). The detection of Ca, K, Mg, and Na confirmed LIBS has sufficient sensitivity as a tool for characterization of paleo-climate proxy indicators in ice. Sample analysis throughput with LIBS was a factor of ten greater than analysis using conventional ICP-MS and required no special sample preparation or use and disposal of hazardous digestion chemicals. We are continuing to work on this project and have designed a new cooling stage to facilitate work with frozen samples.

Though it does not appear in a peer-reviewed journal a book chapter specifically focused on geochemical fingerprinting using LIBS was published in

2014: Richard R. Hark, Russell S. Harmon. Geochemical Fingerprinting Using LIBS, Chapter 12 in Laser-induced Breakdown Spectroscopy: Fundamentals and Applications, Musazzi, S., Perini, U. (Eds.), Springer-Verlag:Berlin, 2014

Though our efforts to obtain a portable LIBS system through grants (e.g., two DURIP proposals were submitted over the last three years) we finally have access to a handheld LIBS instrument as a result of a collaboration with a company (SciAps, Inc.). We plan to reanalyze the same sample suites (cassiterite, columbite-tantalite, obsidian, garnets) to see if the levels of discrimination are similar to those obtained using our laboratory-based instrument.

In summary, our efforts over the last three years have demonstrated that LIBS analysis combined with chemometric data processing is a valuable tool that can be used to better understand the natural geologic background and thereby facilitate identification of geomaterials of interest.

Technology Transfer

None

Chapter 12

Geochemical Fingerprinting Using LIBS

Richard R. Hark and Russell S. Harmon

Geochemical fingerprinting is based upon the idea that the chemical composition of a mineral or rock reflects the geological processes associated with its formation. Information about the elemental composition and isotopic ratios has been used extensively within the geochemical community to differentiate geological samples derived from distinct source reservoirs or having a different post-formation history. Laser-induced breakdown spectroscopy (LIBS) offers an attractive means of distinguishing different geographic sources for a geomaterial in a field setting in real time. The emission spectrum from the microplasma, formed when the laser ablates material from a sample, provides a ‘spectral fingerprint’ of the substance that simultaneously includes all elements. When used in conjunction with chemometric data processing LIBS allows for rapid analysis of materials without the need for sample preparation.

12.1 Geochemical Fingerprinting

A fingerprint is an impression composed of curved lines that is made on a surface by a fingertip. The pattern of ridges provides a unique biometric identification mark that can be used to identify individuals. In a more generic sense, a ‘fingerprint’ can be considered a distinctive or identifying mark or characteristic. The term *geochemical fingerprint* is frequently used in the geosciences to refer to a chemical marker or signal that provides “information about the origin, the formation, and/or the environment of a geological sample” [1]. Its foundation is the understanding that

R. R. Hark (✉)

Department of Chemistry, Juniata College, 1700 Moore Street, Huntingdon, PA 16652, USA
e-mail: hark@juniata.edu

R. S. Harmon

Department of Marine, Earth and Atmospheric Sciences, North Carolina State University,
Raleigh, NC 27695, USA
e-mail: rsharmon@ncsu.edu

geological processes leave behind chemical and isotopic patterns, i.e. ‘fingerprints’, in the geological record [2, 3], provided of course that, once created, the mineral, rock, or other geological material retains its original chemical composition to an extent that this can still be recognized at the time of analysis.

The concept of geochemical fingerprinting is based upon four hypotheses:

1. Minerals form in certain structures according to sets of well-understood rules, depending on the geologic setting.
2. The Earth’s mantle and crust are compositionally heterogeneous, both horizontally and vertically.
3. Minerals forming within a specific geological domain will reflect that inherent spatial heterogeneity.
4. Secondary geological processes acting on a geological material, particularly water–rock interaction at shallow levels in the Earth’s crust, can modify the original geochemical character of a material and produce an overprint geochemical signature that is distinctive and diagnostic in its own right.

Samples of the same mineral formed at different locations (or at nearby locations via separate geologic events) may therefore have dissimilar trace element content or unique isotopic ratios, even though the physical appearance and percentages of major constituents are essentially identical. If sufficiently sensitive chemical composition data can be obtained it may be possible to determine the provenance of a sample by comparison with a library of samples with known origin.

12.1.1 Formation of Minerals: Geology and Geochemistry

Geochemical fingerprints arise because chemical elements partition into solids, liquids, and gasses differently as a function of the bulk composition, temperature, pressure, gas fugacity, and fluid acidity of the system. This is true whether one is considering the melting of the Earth’s mantle or continental crust, two different minerals crystallizing sequentially from a magma, an ore or gangue mineral forming from a hydrothermal or epithermal solution, the dissolution of minerals during water–rock interaction in sediments, the precipitation of minerals from evaporating seawater, the exsolution of carbon dioxide from a petroleum brine, or the formation of ice in a lake. As a consequence, the composition of the more than 3,800 distinct minerals that have been identified on Earth [4] have distinct chemical compositions. Knowledge of the chemical composition of the mineral assemblage present in a rock is critical to understanding its origin and history such as the pressure, temperature, and chemical environment of its formation; the pressure and temperature conditions of any post-formation hydrothermal alteration or recrystallization events; and the extent of weathering at the Earth’s surface.

As modified from Hoefs [1], the various kinds of geochemical fingerprints include those that: (i) have an unusual or anomalous elemental concentration or isotopic composition, (ii) are a group of trace elements that produce diagnostic

elemental patterns on Schoeller-type semi-logarithm diagrams, (iii) contain characteristic organic molecules called ‘biomarkers’ that denote a specific biosynthetic pathway or microbial origin, and (iv) different classes of isotopic composition (e.g., extinct, radiogenic, cosmogenic, or stable) whose present-day composition are a consequence of a specific geological history. Used in this context, the earth sciences community typically uses geochemical fingerprints to recognize specific geochemical reservoirs, within the Earth or on its surface, that create distinctive geological environments (e.g., atmosphere vs. hydrosphere, marine vs. freshwater, biotic vs. abiotic, oxic vs. anoxic, upper crust vs. lower crust, crust vs. mantle) that play a role in the origin of a mineral, rock, or other geological material like sediments and soils.

The concept of a geochemical fingerprint goes back to the time of Victor Morris Goldschmidt, generally considered the ‘father of geochemistry’, who argued that certain chemical elements could be used to reveal genetic relationships among different types of igneous rocks [5]. Today, the concept of geochemical fingerprinting is more expansive and has been used in a very broad spectrum of applications across the earth, environmental, and archeological sciences such as

1. distinguishing and differentiating different mantle compositional reservoirs,
2. recognizing impact events during Earth history,
3. elucidating change in atmospheric character and redox state during the Earth’s early evolution,
4. documenting distinct geological processes at different times during Earth history,
5. discriminating amongst magmatic rocks generated in different geotectonic settings,
6. as pathfinders for different types of ore deposits,
7. discerning waters of different origin,
8. revealing the provenance of different natural and man-made materials,
9. identifying different biosignatures,
10. detecting specific anthropogenic imprints and the identification of natural backgrounds that can be used in the identification of toxic metal contamination in the environment.

For example, the volcanic rocks generated along the spreading centers of the world’s ocean basins (mid-ocean ridge basalts), those generated at mid-plate ocean islands like the Azores, Hawaii and Tahiti (ocean island basalts), and those erupted at the margins of subduction zones like those characteristic of the ‘Pacific Ring of Fire’ (island arc basalts), each have a distinctive chemical signature when normalized to the composition of the primitive mantle [6]. Many studies have shown that the glass matrix of tephra and ignimbrites can be used to geochemically fingerprint the volcanic source and individual eruptive events [7–11]. Similarly, granites emplaced into the continental crust in different tectonic settings can be recognized on the basis of their distinct chemical signatures [12] as can the xenoliths found in continental basalts [13]. Detrital zircons in supracrustal sediments [14] have distinctive chemical signatures that permit the recognition of

different lower crustal terranes of different geologic age as well as insight into subduction and cumulate processes in the earth's deep interior [15]. It is important to note that geochemical fingerprints can be manifest on all spatial scales, from the very smallest micron scale zoning within a mineral to the global scale of distinct compositional reservoirs in the Earth's mantle.

Mineral deposits unevenly distributed through the Earth's history and particular classes of deposits are restricted to narrow intervals over geological time. This situation and the resultant patterns of ore deposit distribution observed reflect direct links between the long-term geodynamic cycles that control styles of heat flow and consequent magmatism and associated metallogenic processes. Prospecting for mineral deposits often relies on the concept of geochemical fingerprinting. In some cases this may involve the recognition of a key chemical signature in minerals called 'pathfinders'. For instance, kimberlitic diamonds are commonly associated with significantly more abundant Cr-diopside pyroxenes and garnets with high Cr/Ca ratios [16]. Many rock units exhibit spatial variations in mineral composition that provide clues to the processes that formed or recrystallized the rock. For example, banded iron formation, porphyry skarn, volcanogenic massive sulfide, and porphyry vein type deposits exhibit compositional differences that can be related to deposit types, and their geochemical fingerprints can be used to separate different styles of mineralization [17]. Arsenic variations in geothermal sinters (amorphous silica) can act as a guide to gold enrichment [18]. Also, multi-element analysis of detrital and ore minerals can be used to discriminate different types of mineral deposits [17] and to determine ore mineral provenance [19–23].

Certain types of types of naturally occurring gases have a genetic association with particular types of orebodies and ore-bearing intrusions. Some of their chemical components can be used as exploration pathfinders [24]. Likewise, groundwaters can interact with ore deposits and thus their chemical signatures can be employed to prospect for different styles of mineralization, including porphyry copper, volcanogenic massive sulfide, sandstone-hosted uranium, and gold deposits [25].

Chemical fingerprinting of natural waters [26–29], both marine and terrestrial sediments [30–34], atmospheric dust [35, 36], and oil and petroleum products [37–40] undertaken on the basis of their trace element content is well established. Similarly, in the archaeological field, the approach of chemical fingerprinting has been used to determine the source areas of rock artifacts, ceramics, cultural glass, obsidian artifacts, ancient coinage, and natural gemstones [41–56].

12.1.2 Elemental Analysis Techniques for Geochemical Fingerprinting

Information about the elemental composition and isotopic ratios present in a mineral has been used extensively within the geochemical community to discriminate geological specimens originating in one place from samples of the same

kind from other locations. Over the past thirty years, many different analytical techniques ranging from X-ray diffraction and fluorescence spectrometry (XRD & XRF), electron microprobe analysis (EMP), and instrumental neutron activation analysis (INAA), to inductively-coupled plasma analysis and mass spectrometry (ICP & ICP-MS), mass spectrometry (MS), and laser-ablation inductively-coupled plasma mass spectrometry (LA-ICP-MS) have been utilized within the earth, environmental, and archaeological sciences communities for geochemical fingerprinting [2]. Some of these techniques can be performed directly on untreated solid samples, whereas others utilize liquid analytes and therefore require sometimes extensive sample preparation, such as repetitive microwave-assisted acid digestion. No one technique does everything well, so evaluation of which analytical approach to use for geochemical fingerprinting necessitates that other factors such as accuracy, precision, sensitivity, throughput, sample consumption, ease of use, cost per analysis, and portability must be taken into account (see Table 12.1).

For example, EMP is a convenient technique that is used routinely for analysis of geomaterials, but the limits of detection (LOD) may not be low enough to discriminate between similar samples, and the instrumentation is very expensive. XRF is comparable to EMP in terms of performance but has the advantage that handheld systems are available for field use. INAA has excellent sensitivity, on the order of parts per billion, but the technique is costly, takes a long time, provides simultaneous analysis only for approximately 30–40 elements at a time, requires working with high levels of radiation, and cannot be used to analyze for certain elements (e.g., Ba, Sr, and Zr) present in abundance in many geological samples. Though INAA is technically considered to be non-destructive, analyzed samples can remain radioactive for years [58]. Measurement of light elements ($N < 8$) is problematic for all of the aforementioned methods. Even a ‘gold standard’ technique such as LA-ICP-MS—which has excellent sensitivity, precision and accuracy, is minimally destructive, requires little sample preparation, and is fast—has drawbacks, such as the very high cost of the system, the clean room environment necessary to achieve maximum analytical performance, the consumable chemicals utilized in the sample preparation, the complexity of using the instrument, and the fact that it is not amenable for use in the field [57].

12.2 LIBS for Geochemical Fingerprinting

Laser-induced breakdown spectroscopy (LIBS) is a straightforward atomic emission spectroscopic technique that can provide rapid, multi-element detection in real-time with minimal sample preparation. As documented by the steady increase in the number of “GeoLIBS” publications appearing in peer-reviewed journals (Fig. 12.1), LIBS is being increasingly applied to the analysis and provenance verification of geomaterials [56]. An attractive feature of LIBS, which has not yet been fully exploited, is that it can be readily implemented in the laboratory, in industrial facilities, or in the field for close-in analysis or at stand-off distances

Table 12.1 A comparison of analytical figures of merit for techniques used for geochemical analysis (adapted from Naes et al. [57])

| Parameter | EMP | XRF | INAA | LA-ICP-MS | LIBS |
|----------------------------------|---------------------|---------------------|-------------------------|-----------------------|-----------------------|
| <i>Accuracy</i> | Semi-quantitative | Semi-quantitative | Quantitative | Quantitative | Semi-quantitative |
| <i>Precision RSD</i> | Good (5–10 %) | Good (5–10 %) | Good-excellent (~ 5 %) | Excellent (<5 %) | Fair-good (5–10 %) |
| <i>Sensitivity</i> | 100's ppm | 100's ppm | ppb | < 1 ppm | 10s ppm |
| <i>Discrimination</i> | Very good-excellent | Very good-excellent | Very good | Excellent | Very good-excellent |
| <i>Complexity</i> | Easy to use | Easy to use | Fairly difficult to use | Difficult to use | Very easy to use |
| <i>Sample Consumption</i> | Non-destructive | Non-destructive | Non-destructive | Minimally destructive | Minimally destructive |
| <i>Throughput (per analysis)</i> | Minutes | Minutes | Hours | Minutes | Seconds |
| <i>Cost (USD)</i> | ~\$700K | \$75–150K | ~\$100K | ~\$250K | \$75–\$150K |

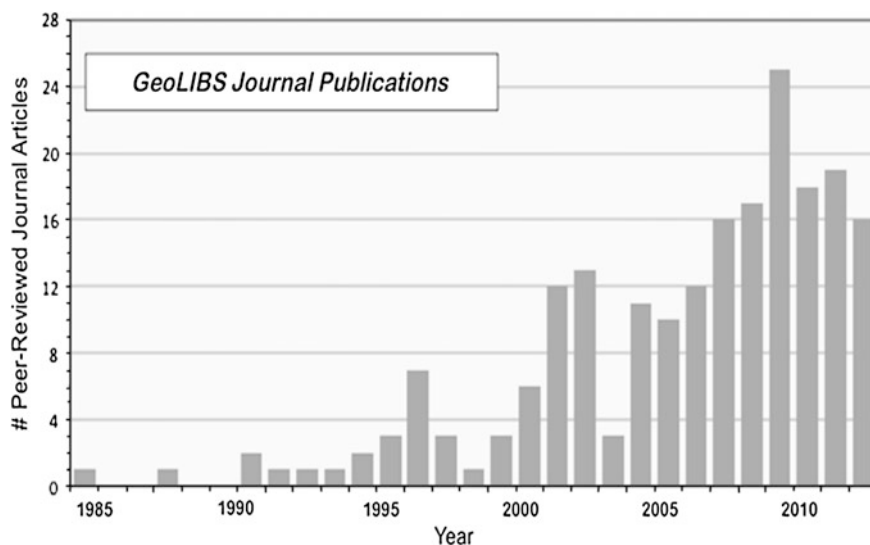


Fig. 12.1 Histogram showing the number of papers appearing in peer-reviewed journals since 1984 that relate to analysis of geological or environmental materials using LIBS

exceeding 100 m for both elemental detection and quantitative chemical analysis. The instrumentation is robust, as demonstrated by the deployment of a LIBS system as a component of the *ChemCam* science package on the Mars rover *Curiosity* [59]—a spectacular example of extraterrestrial geochemical analysis.

For the LIBS technique, a high-intensity pulsed laser is focused on the surface of a sample to create a microplasma. Light is emitted at discrete wavelengths as the plasma cools and the electrons of atoms and ions in excited electronic states return to the ground states. Since every element in the periodic table has one or more emission lines in the UV, visible and near IR region portion of the spectrum (200–900 nm) and emission intensity is proportional to the concentration of the emitting species, a unique LIBS spectral signature—a *geochemical fingerprint*—can be obtained for a geological sample. See Part 1 for additional details on LIBS fundamentals.

12.2.1 LIBS Instrumentation

LIBS instrumentation consists of several components that can be configured for laboratory experimentation or reduced in size and ruggedized for field use. Typical LIBS systems utilized for geochemical analysis consist of (i) a Q-switched Nd:YAG nanosecond laser operating at 1,064 nm (or one of its frequency multiplied harmonics) that is used to create a microplasma on the sample, (ii) optics to focus the laser light onto the target and to collect the light emitted as the plasma

cools, (iii) a spectrograph (e.g., Czerny-Turner, echelle) and detector (e.g., CCD, ICCD) for acquisition of the spectrum, and (iv) a computer for system control and data processing. The choice of system components determines performance metrics such as the spectral line intensities, range and resolution, and the degree of laser-matrix coupling. These and other factors influence the appearance of the spectra and this can affect the quality of the geomaterial classification results. For example, comparison of LIBS spectra of silicate glasses such as obsidian obtained using a laser operating at 266 nm with those generated with a 1,064-nm laser reveals large differences in emission line intensities due to differential coupling of the laser with the matrix (see Fig. 12.2), but the classification performance is similar for both approaches [60, 61].

LIBS systems can be assembled in a variety of configurations depending on the requirements of the analytical task. Instruments can be designed for close-in analysis using a sample chamber or a short umbilical probe, or for stand-off detection at a distance. Although most geochemical fingerprinting studies have employed single-pulse configurations, double-pulse arrangements have been utilized in some cases [61, 62]. Most LIBS instruments utilize gated spectrometers so that continuum radiation can be excluded from the spectrum but non-gated systems have been used with success in certain instances [63]. The LIBS emission can also be further enhanced by analysis in an inert gas atmosphere such as He or Ar. Commercial turnkey LIBS systems with data acquisition and processing software are available from several manufacturers in a variety of configurations.

12.2.2 Advantages and Disadvantages of LIBS for Geochemical Fingerprinting

LIBS provides rapid, high-volume, and in situ chemical analysis in real time in both conventional laboratory settings and in the field. Specifically, it offers several important advantages that make it a useful analytical technique for geochemical materials, especially in comparison to existing methods (Table 12.1):

1. LIBS has the potential to detect all elements in a geomaterial with a single laser pulse when the system is configured with a broadband spectrometer.
2. Unlike many other common techniques (see Sect. 12.1.2) that are laboratory based and often require complex and time consuming procedures, LIBS requires little to no sample preparation.
3. LIBS instrumentation is less expensive to acquire and has lower subsequent operating costs than many other techniques.
4. The LIBS technique is particularly sensitive to light elements (H, Li, Be, B, C) that are often a component of geological samples but are problematic to determine by many other analytical techniques. Quantitation of N and O is also possible if the analysis is performed in non-ambient atmosphere [64].

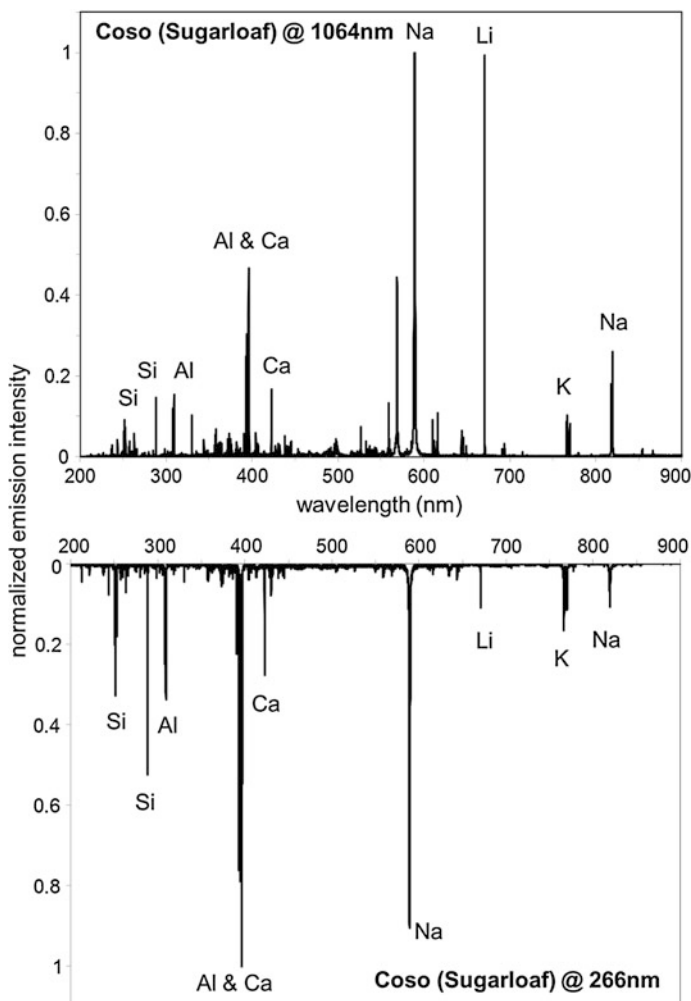


Fig. 12.2 LIBS spectra of the same obsidian sample (Coso Volcanic Field—Sugarloaf Mountain) obtained with a 1,064 nm Nd:YAG laser (*top*) and a frequency quadrupled Nd:YAG laser operating at 266 nm (*bottom*) showing that shorter wavelengths couple better with the silicate matrix

5. LIBS provides high lateral spatial resolution (10–100 s of microns), thus allowing for in situ analysis of individual particles, mineral grains, or inclusions [65, 66] or the fine-scale compositional mapping of a complex sample such as a chemically zoned mineral [67, 68]. Stratigraphic analysis is possible since a crater forms that progressively bores down into a sample with successive laser pulses [69–71].
6. LIBS analysis consumes only nanograms of material per laser pulse and, therefore, can be considered minimally destructive.

7. Other complementary spectroscopic techniques, such as Raman spectroscopy [72] and laser-induced fluorescence (LIF) [73, 74], can be conveniently combined with LIBS to permit simultaneous, orthogonal, multi-elemental analysis. For example, a combined stand-off system has been used to collect both Raman and LIBS spectra of various common minerals [72, 75].

Like all analytical techniques, LIBS suffers from certain disadvantages that must be understood and taken into account when carrying out geochemical fingerprinting experiments. The limits of detection (~ 10 s of ppms) and the level of precision (typically 5–20 % RSD) for LIBS experiments are generally not as good as some established methods used for analysis of geomaterials but are often sufficient to provide discrimination between samples of different provenance. Some elements with high ionization potentials (e.g., F, Cl, and S) have higher LOD's, but emission intensities can be enhanced for weaker lines by carrying out the analysis in an inert atmosphere such as He or Ar. The drawbacks of the LIBS technique are principally related to matrix effects and shot-to-shot variability due to the inherent uneven energy distribution of a nanosecond laser pulse and the differential coupling of the laser energy to the sample surface from one shot to the next.

Physical matrix effects occur due to variability in the composition, grain size, texture, reflectivity, and hardness of the surface of a geomaterial. For example, the magnitude of laser energy coupling with the surface and resultant intensity of the LIBS signal generated is influenced by the roughness of the surface [76, 77]. The influence of matrix inhomogeneities can be ameliorated by homogenization of the sample (though this nullifies one of the main advantages of LIBS), utilization of an algorithm to reject anomalous spectra that are non-representative of the bulk sample, or, more commonly, interrogation of the sample with hundreds or even thousands of laser pulses distributed in a grid pattern [78].

Chemical matrix issues arise when one element influences the emission behavior of another element. For example, an element present in equal concentration in two different host materials will exhibit different LIBS emission intensities [79, 80]. This makes it very challenging to find matrix-matched standards with which to perform quantitative LIBS analysis of natural samples. However, this phenomenon can actually contribute constructively to the uniqueness of the LIBS spectra for a particular sample and may thereby enhance qualitative discrimination. Quantitative analysis of geomaterials is possible with LIBS using either internal or external calibration procedures [81] and calibration-free LIBS approaches have been studied extensively, which eliminates the need for constructing calibration curves [82–85].

The inherent shot-to-shot variability in LIBS experiments is associated with the uneven energy distribution of the nanosecond laser pulses that are most commonly used for ablation and the complex, non-linear processes involved in the coupling of the laser with the matrix [86]. The problems associated with poor precision can be diminished by ensemble averaging [87] or by normalizing the data with respect to the emission intensity of a line associated with a major component [88]. Moreover, spectra from the same sample collected on different LIBS instruments

cannot be assumed to be identical. The strong dependence of LIBS spectra on the specific system components and configuration means that spectral libraries created using one LIBS instrument may not necessarily be transferable without employing some type of transformation algorithm.

12.2.3 Data Acquisition and Multivariate Data Analysis

Acquisition of a large quantity of LIBS data in a short period of time is easy to accomplish—the greater challenge is to obtain high quality, information-rich spectra and then to process that information quickly and efficiently to answer questions of identification or geochemical provenance. The first step in the process is to optimize experimental parameters such as laser wavelength and energy (to maximize laser-matrix coupling and avoid saturation and line broadening), spectrometer gate delay and width (to enhance the intensity of the emission lines versus the continuum background), and sampling protocol (to ensure adequate representation of the chemical composition of the sample using averaging or accumulation of spectra). Optimization is typically done simply by adjusting parameters to improve the signal-to-noise ratio (S/N) of weak emission lines, though it is possible to explore “parameter space” empirically to provide maximum discrimination between multiple samples as determined by various chemometric techniques. It is frequently necessary to use several laser pulses to clean a mineral sample in order to remove surface contamination, alteration, or oxidation layers.

Differences between the LIBS spectra of minerals or rocks of significantly dissimilar composition are usually readily discernible by visual inspection. However, geochemical fingerprinting frequently relies on small differences in the amounts of minor or trace elements present in the sample to effect discrimination and establish a unique provenance for geomaterials of similar composition. Multivariate analysis is a technique used to reduce or compress the multi-dimensional spectral data into fewer combinations of variables that still retain the essential information describing the data set. For this reason chemometric approaches, ranging from simple linear correlation analysis [89] to more complex multivariate techniques, are often required to discriminate between similar geological samples [90]. Principal component analysis (PCA) [91] and partial least squares discriminant analysis (PLSDA) [22, 23, 62] are two common chemometric techniques that have been used extensively with LIBS for geochemical fingerprinting, but many other methods, such as artificial neural networks (ANN) [92–94] and soft independent modeling of class analogy (SIMCA) [95, 96], can be utilized.

PCA is an unsupervised statistical analysis technique that reduces the complexity (dimensionality) of the data by finding linear combinations of variables (i.e. principal components) that explain the differences between samples [86]. This type of exploratory data analysis provides a graphical representation of the natural grouping of the samples and highlights which variables (i.e. emission wavelengths)

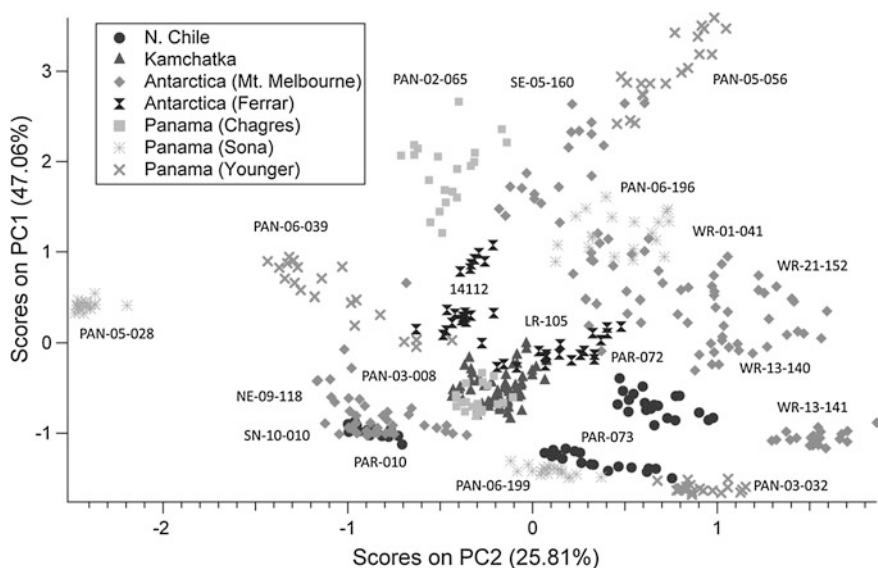


Fig. 12.3 Scores plot of principal component 1 (*PC1*) versus principal component 2 (*PC2*) for the principal component analysis (*PCA*) model built using 400 LIBS spectra from 20 different volcanic rock samples obtained from seven locations in Antarctica, Chile, Panama, and Antarctica

most strongly influence the clustering. Spectral preprocessing, such as normalization followed by mean-centering, is typically employed to improve the quality of the results. *PCA* scores are linear combinations of the original variables and describe how the samples relate to each other while *PCA* loadings contain information about how the variables relate to each other. The first few *PCA* loadings usually explain most of the covariance between samples. Figure 12.3 illustrates how a two-dimensional *PCA* scores plot graphically displays the degree of clustering of spectra from the same sample and the separation between samples from different locations.

PLSDA is a supervised inverse least-squares approach in which an algorithm with predictive latent variables is generated that maximizes the variance between spectra collected from samples having different geographic origins. Once it has been trained, the model can then be used to predict the probability that spectra from a new sample belong to a previously identified class. A reasonable number of examples (ideally 5–10) should be available for each class so that a portion can be used to train the model and the remainder of samples reserved to test the performance of the model.

PLSDA data is frequently displayed in the form of a ‘confusion matrix’ (Table 12.2). The model classes represent the geographic identifier (e.g., sample, mine location, region, country) to which each of the spectra was assigned prior to building the *PLSDA* model. The algorithm then places each of the spectra being

evaluated into one of the model classes. Correct classification corresponds to the values found along the diagonal while values in off-axis cells correspond to misclassifications.

PLSDA has proven to be a very effective technique for geochemical fingerprinting because it maximizes the inter-class variance (i.e. provenance) while minimizing the intra-class variance (i.e. shot-to-shot variability). However, in order to ensure robustness the model must be cross-validated using one of several approaches. In k -fold cross-validation, for example, one group of spectra is sequestered and the remaining groups are used to develop a model for classification; the classification model is then applied to the sequestered group of spectra to estimate labels. The process is re-run for k iterations until each group of spectra serves as the reserved test set. Cross-validation schemes, such as leave-one-sample-out (LOSO), that divide groups based on samples rather than individual spectra, have been shown to provide more robust results than k -folds cross-validation [97], but these can only be used when there are at least two samples for each model class.

Model performance will be affected by factors such as data pre-processing (e.g., normalization), the number of input variables (i.e. selected emission lines or the whole spectrum), the number of classes and how many samples are in each class, and the number of latent variables. Caution should be exercised since PLSDA models are subject to “over-training”, which can lead to erroneously favorable results, especially if small sample suites are used with only two or three class designations.

The input for PLSDA analysis can be either selected emission lines or the entire broadband LIBS spectrum. The former approach may be favored when information on the chemical composition of a sample suite provides insight into which lines to include in the PLSDA model. The latter avenue requires no prior knowledge of the chemistry of the samples, but the inclusion of baseline noise, which does not contribute to discrimination, increases the complexity of the calculations and may reduce the classification performance. In a study involving an obsidian sample suite, the use of individual emission lines gave approximately 10 % better results on a sample-level classification task than use of the full broadband spectrum consisting of over 13,000 wavelengths [98]. However, when samples from the same location were grouped together, the location-level classification performance was comparable for both approaches. Though no definitive conclusions can be drawn from this example, the PLSDA algorithm is frequently able to extract the features useful for discrimination and ignore the useless wavelengths. Preprocessing steps that eliminate noise (e.g., removal of features that show low statistical co-variance between all of the spectra in the model) or identify significant emission lines (e.g., use of principal components derived from PCA analysis as features) may also improve PLSDA performance and shorten computational time. The latter benefit would be especially advantageous when the technique is utilized for real-time analysis in the field. Given the relative ease of developing PLSDA models, empirical comparison of multiple methods is prudent.

Table 12.2 Confusion matrix for classification of 38 samples of cassiterite ore concentrate (principally SnO₂) from 11 locations in South America and Asia generated from a PLSDA analysis using 10-fold cross validation. The overall rate of correct classification is 87 %

| Test Sample (country/ source) | # of Spectra | Model classes | | | | | | | | | | Taboca | MSC |
|---|-----------------|---------------|-----------|-----------|---------|--------|--------|-----------|--------|--------|-----------|-----------|-----|
| | | Morocola | Caracoles | Colquiri | Huanuni | Oruro | Minsur | Thaisarco | Mentok | Kundur | | | |
| <i>Bolivia</i> (<i>Morocola</i>) | 100 | 83 (83 %) | 11 | 0 | 1 | 1 | 0 | 3 | 0 | 1 | 0 | 0 | 0 |
| <i>Bolivia</i> | 100 | 0 | 100 | 0 | 0 | 0 | 0 | 0 | 0 | 0 | 0 | 0 | 0 |
| (<i>Caracoles</i>) | | | (100 %) | | | | | | | | | | |
| <i>Bolivia</i> | 100 | 0 | 0 | 99 (99 %) | 0 | 0 | 1 | 0 | 0 | 0 | 0 | 0 | 0 |
| (<i>Colquiri</i>) | | | | | | | | | | | | | |
| <i>Bolivia</i> | 400 | 0 | 0 | 0 | 382 | 14 | 1 | 1 | 1 | 1 | 0 | 0 | 0 |
| (<i>Huanuni</i>) | | | | | (96 %) | | | | | | | | |
| <i>Bolivia (Oruro)</i> | 1200 | 6 | 13 | 17 | 87 | 853 | 53 | 46 | 55 | 43 | 0 | 27 | |
| | | | | | | (71 %) | | | | | | | |
| <i>Peru (Minsur)</i> | 900 | 0 | 1 | 8 | 6 | 11 | 848 | 8 | 3 | 15 | 0 | 0 | 0 |
| | | | | | | | (94 %) | | | | | | |
| <i>Thailand</i> (<i>Thaisarco</i> <i>smelter</i>) | 400 | 3 | 2 | 2 | 6 | 6 | 9 | 361 | 6 | 4 | 1 | 0 | 0 |
| | | | | | | | | (90 %) | | | | | |
| <i>Indonesia</i> (<i>Mentock</i>) | 200 | 1 | 0 | 0 | 0 | 2 | 0 | 3 | 189 | 5 | 0 | 0 | 0 |
| | | | | | | | | | (95 %) | | | | |
| <i>Indonesia</i> (<i>Kundur</i>) | 200 | 0 | 0 | 0 | 1 | 1 | 1 | 1 | 10 | 184 | 1 | 1 | 1 |
| | | | | | | | | | | (92 %) | | | |
| <i>Brazil (Taboca)</i> | 100 | 0 | 0 | 0 | 1 | 2 | 0 | 0 | 0 | 0 | 97 (97 %) | 0 | 0 |
| <i>Malaysia (MSC</i> <i>smelter)</i> | 100 | 0 | 0 | 0 | 1 | 3 | 1 | 1 | 0 | 0 | 0 | 94 (94 %) | 0 |

12.3 Examples of Geochemical Fingerprinting Using LIBS

With typical LIBS instrumentation, a single laser pulse allows acquisition of the broadband emission spectrum from approximately 200–900 nm. Such broadband LIBS spectra contain all the chemical information about the sample and, therefore, provide a unique chemical signature of the material (Fig. 12.4). The broadband LIBS spectrum for a specimen of common beryl ($\text{Be}_3\text{Al}_2\text{Si}_2\text{O}_6$) from Antarctica is shown in Fig. 12.5. Pure beryl is colorless, however, the presence of trace elements in the mineral structure can yield the green, blue, yellow, and red varieties valuable as gem minerals. Because of this potential for diverse elemental substitution, many minerals, like beryl, reliably acquire a chemical fingerprint from their environment during formation. Thus, LIBS can be used to identify minerals as well as determine their provenance in circumstances where the minerals have formed within different geochemical environments. The additional examples described in the succeeding section are not exhaustive but serve to illustrate the principles of LIBS-based geochemical fingerprinting.

12.3.1 Common Minerals

As previously noted, minerals are the basic building blocks of solid earth materials, whether rocks, sediments, or soils. Identification of the chemical composition of the mineral assemblage present in a geological sample provides a wealth of information about its origin and history, such as the pressure, temperature, and chemical environment of its formation; the pressure and temperature conditions of any post-formation hydrothermal/epithermal alteration or recrystallization events; and the extent of its weathering at the Earth's surface.

Most commonly, mineral identification in the field is based on a physical property like crystal habit, color, streak, magnetic character, acid solubility, etc., but even the experienced field geologist may find it difficult to distinguish fine-grained minerals or minerals having similar physical properties. This is particularly true for complex minerals like garnet, pyroxene, amphibole, feldspar, beryl, and tourmaline that are members of multiple solid solution series and thus have multiple possibilities for elemental substitution in the mineral structure. A portable LIBS instrument represents an attractive possibility for real-time chemical analysis of minerals in the field.

Another advantage of LIBS, compared to other analytical techniques used for in-field chemical analysis such as X-ray fluorescence and Raman spectroscopy, is its capability to analyze elements of low atomic number. The mineral tourmaline, which has one of the most complex and variable chemical formulas of all minerals, illustrates the benefit of being able to identify light elements (i.e., Li, Be, and B) in a mineral sample. Rather than being a single mineral of fixed composition like quartz (SiO_2), gypsum ($\text{CaSO}_4 \cdot 2\text{H}_2\text{O}$) or topaz ($\text{Al}_2\text{SiO}_4[\text{F,OH}]_2$), tourmaline is a name

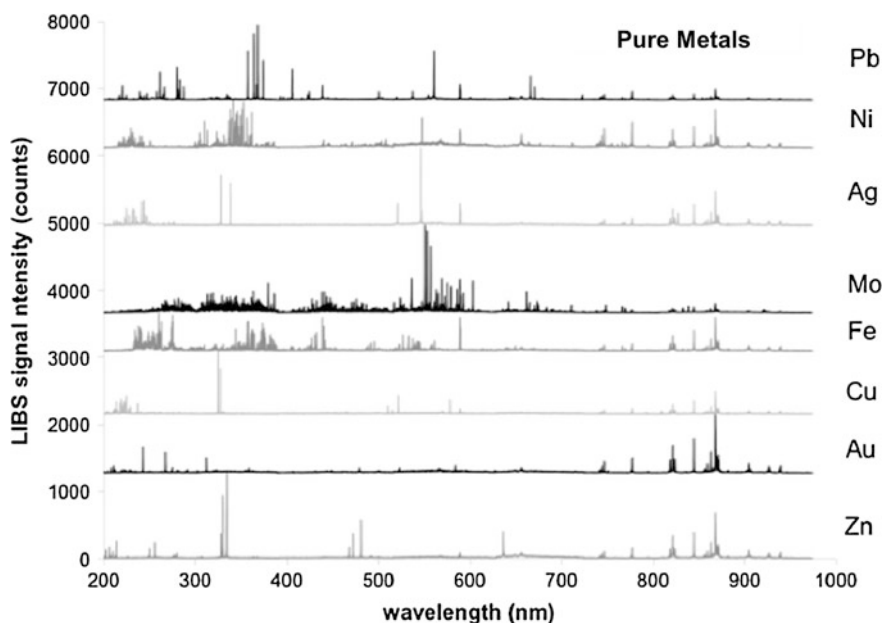


Fig. 12.4 Single-shot, broadband LIBS spectra for eight pure metals (Ag, Au, Cu, Fe, Mo, Ni, Pb, and Zn) illustrating that every element has a unique LIBS spectrum [77]

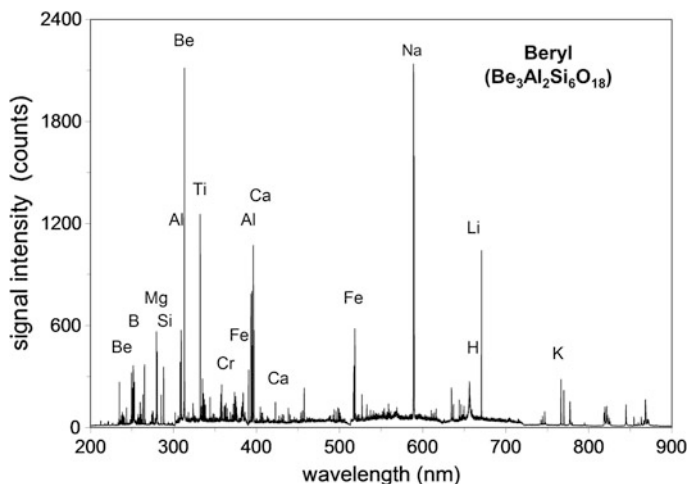


Fig. 12.5 Broadband, single-pulse LIBS spectrum for a specimen of common beryl ($\text{Be}_3\text{Al}_2\text{Si}_6\text{O}_{18}$) from Antarctica which demonstrates that substitution of trace elements (e.g., Li, B, Na, Mg, K, Ca, Ti, Cr, and Fe) in the mineral structure can be observed using LIBS. Many minerals, like beryl, reliably acquire a chemical fingerprint from their environment during formation

given to a group of 25 isomorphous minerals having the same crystal structure, but distinct chemical compositions [4]. The general chemical formula for tourmaline is $XY_3Z_6(T_6O_{18})(BO_3)_3V_3W$, where $X = Ca, Na, K$; $Y = Li, Mg, Fe^{2+}, Mn^{2+}, Zn, Al, Cr^{3+}, V^{3+}, Fe^{3+}, Ti^{4+}$; $Z = Mg, Al, Fe^{3+}, Cr^{3+}, V^{3+}$; $T = Si, Al, B$; $B = B$; $V = OH, O$; and $W = OH, F, O$. The three most common end-member varieties of tourmaline, which normally cannot be distinguished except by chemical analysis, are:

1. schorl ($NaFe_3^{2+}Al_6[BO_3]_3Si_6O_{18}[OH]_4$),
2. dravite ($NaMg_3Al_6[BO_3]_3Si_6O_{18}[OH]_4$), and
3. elbaite ($Na[Li, Al]_3Al_6[BO_3]_3Si_6O_{18}[OH]_4$).

A broadband LIBS spectrum for the two portions of a common ‘watermelon’ tourmaline specimen with repetitive green and pink zoning is shown in Fig. 12.6. As discussed by Harmon et al. [58], the presence of strong Li and Al peaks, but only a minor Fe peak, shows that this tourmaline lies toward the schorl–elbaite end of the compositional spectrum. The alternating green-to-pink zoning of the tourmaline was attributed to Mg and Mn variations in the trace element chemistry of the parent hydrothermal solutions from which it formed, with the pink zones developing when the hydrothermal fluids became enriched in Mn and the green tourmaline crystallizing from solutions alternatively enriched in Mg.

The study of McMillan et al. [100] demonstrated that different carbonate and silicate minerals could be readily discriminated on the basis of their LIBS broadband spectra, illustrating the first, simple application of the geochemical fingerprinting concept. A collection of carbonates, pyroxenes and pyroxenoids, amphiboles, phyllosilicates, and feldspars were interrogated to produce a database containing composite broadband spectra based on averages of 10 laser pulses. All 52 minerals were correctly classified using correlation coefficients resulting from the regression of pairs of LIBS spectra. When the spectrum of each sample was compared to a database containing the other 51 minerals, 65 % were identified as a mineral of similar composition from the same mineral family. Misclassifications occurred either when the mineral had high concentrations of an element not present in the database or in cases where the mineral was misidentified as a mineral with similar elemental composition but belonging to a different family (e.g., dolomite ($[CaMg(CO_3)_2]$) was incorrectly identified as diopside ($[CaMg]Si_2O_6$)).

12.3.2 Geomaterials

The concept of geochemical fingerprinting for determination of provenance is based upon the hypothesis that the chemical composition of a natural material directly reflects the geological environment of its place of formation. This approach can be applied to determining the provenance of volcanic glasses, minerals, and rocks. Conceptually, it is based upon the fact that the Earth’s crust, both horizontally and vertically, is composed of mixtures of rocks of different composition and that

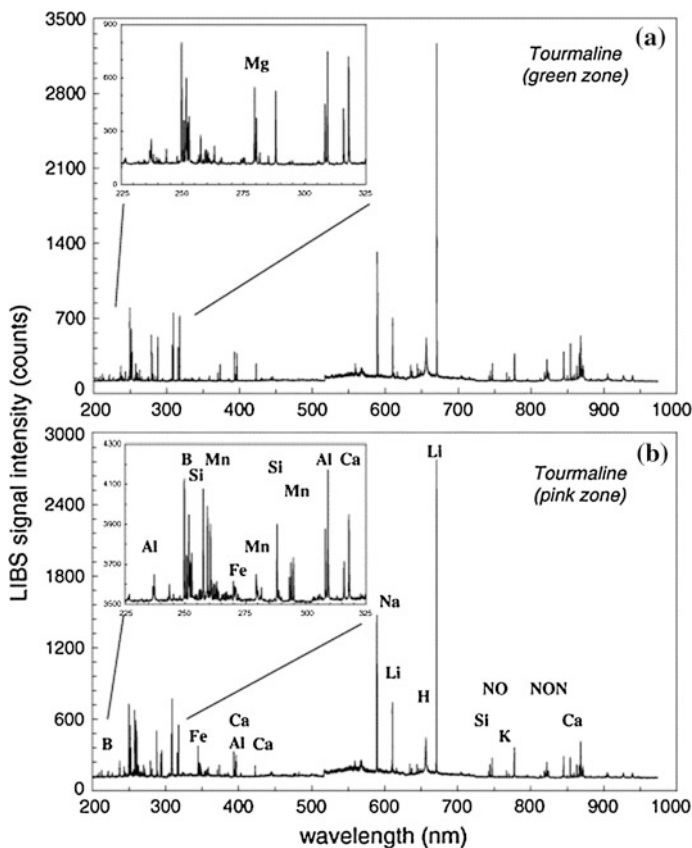


Fig. 12.6 Single-pulse broadband LIBS spectra for a ‘watermelon’ tourmaline specimen exhibiting alternating green and red bands. The LIBS spectra document (i) the presence of the light elements Li and B in the tourmaline and (ii) that the major difference between the two spectra is the presence of Mg in the *green* zone (a) and Mn in the *pink* zone (b). Note that emission lines for N and O from the air are also present [99]

(i) magmas originating in the crust, will directly inherit the chemical signature of that crust; (ii) magmas passing through the crust will interact with it and acquire a chemical signature from the crust; and (iii) pegmatitic and mineralizing fluids moving within the crust will impart a crustal chemical signature to any minerals formed from the fluid. Therefore, provided that a robust LIBS compositional library can be created, it should be possible to determine the place of origin (i.e. provenance) of a geological sample from its broadband LIBS spectrum using advanced multivariate statistical signal processing techniques.

Harmon et al. [77, 89, 99] and Gottfried et al. [62] investigated the potential of using the full broadband LIBS spectrum for a variety of earth and environmental sciences applications, by analyzing minerals, marine biological precipitates, volcanic glasses, rocks, and soils. The idea in applying the concept of geochemical

fingerprinting in LIBS analysis is that the broadband LIBS emission can be used, for example, to discriminate a specific geological specimen from other specimens of the same type [50, 53, 76, 100], to reveal the provenance of minerals, rocks, volcanic glasses [22, 23, 54], to perform rock unit stratigraphic correlation [95], to undertake geochemical mapping [77], and to detect environmental contamination [63].

Other studies have examined the potential to distinguish simple geomaterials using LIBS. Gottfried et al. [62] analyzed a broad suite of more than a hundred natural carbonate, fluorite, and silicate minerals and other geological materials covering a broad compositional and textural range using three different LIBS systems: a commercial single-pulse LIBS system, a laboratory bench-top double-pulse LIBS system, and a prototype stand-off LIBS system with samples at a distance of 25 m. LIBS spectra, produced from the three systems using Nd:YAG laser excitation at 1,064 nm, show distinct differences in the observed emission lines and relative intensities due to differences in laser pulse energy and spectrometer channel sensitivity, although the same elemental species were present in the spectra acquired by all three systems. Even though many more emission lines were observed in the spectra, the laboratory double-pulse LIBS system did not provide significant improvement over the single-pulse LIBS system in the statistical classification results for most of the sample types studied. In one experiment, broadband LIBS spectra were acquired with the laboratory single-pulse Nd:YAG laser at 1,064 nm for a suite of CaCO_3 rocks and minerals that included marbles, sea shells, calcite crystals, and aragonite samples. Although the broadband spectra for the different samples are similar, close inspection of the spectra revealed intensity differences that are a consequence of both matrix effects and the presence of the trace element impurities which determine the color of certain samples. In a second carbonate experiment, single-pulse spectra were collected for 11 different common metal carbonate minerals (Fig. 12.7) and PCA was used to readily distinguish these minerals, from each other and from the calcium carbonate samples calcite and aragonite, on the basis of characteristic metallic emission lines for the cations.

12.3.3 Gemstones

Geochemical fingerprinting of gemstones is used by archeologists, gemologists and geologists to help determine the provenance of mineral specimens. The amounts of minor and trace elements incorporated into a precious or semi-precious mineral species will be affected by the geological conditions in which it is formed; and this frequently determines not only the color of the gemstone but also its value. The origin of a gemstone can be traced to a geological-genetic environment or, more specifically, to a country, geographic locale or even a particular mine. Techniques such as Fourier transform infrared spectroscopy (FTIR), Raman spectroscopy, ultraviolet–visible spectroscopy (UV–Vis), energy dispersive X-ray fluorescence spectroscopy (EDXRF), laser ablation inductively coupled plasma mass spectrometry (LA-ICP-MS), and secondary ion mass spectrometry (SIMS)

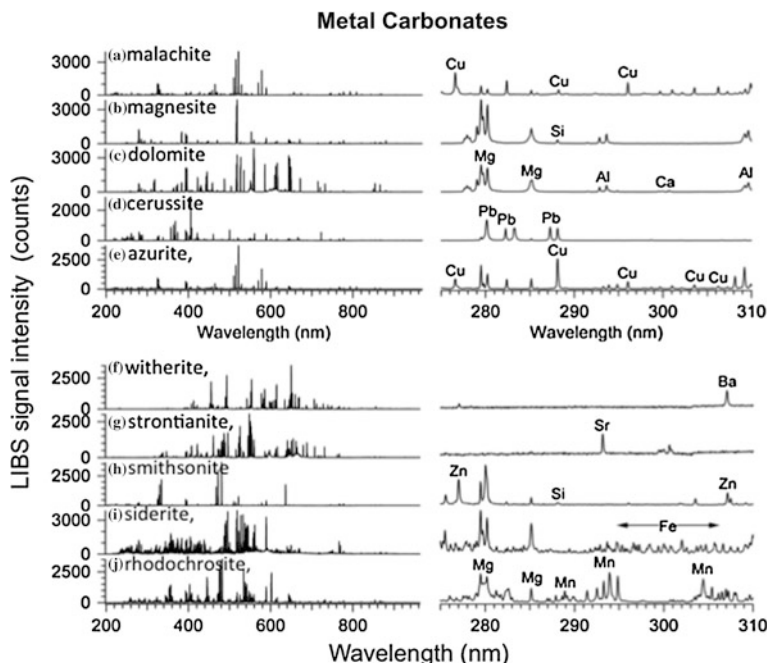


Fig. 12.7 Single-pulse LIBS spectra for 10 end-member metal carbonate minerals: **a** malachite $\text{Cu}_2\text{CO}_3(\text{OH})_2$; **b** magnesite MgCO_3 ; **c** dolomite $\text{CaMg}(\text{CO}_3)_2$; **d** cerussite PbCO_3 ; **e** azurite $\text{Cu}_3(\text{CO}_3)_2(\text{OH})_2$; **f** witherite BaCO_3 ; **g** strontianite SrCO_3 ; **h** smithsonite ZnCO_3 ; **i** siderite FeCO_3 ; and **j** rhodochrosite MnCO_3 . The inset shows the high-resolution portion of each spectrum from 275 to 310 nm in which the cation compositions of the different metal carbonate minerals are identified (modified from Gottfried et al. [62])

have been used to obtain the spectral fingerprints of gemstones [101]. Rapid, reliable chemical analysis of specimens is desirable to both classify genuine gemstones and identify artificially enhanced counterfeit stones—a persistent problem that plagues the legitimate gem industry [102, 103].

12.3.3.1 Beryl

Beryl ($\text{Be}_3\text{Al}_2\text{Si}_6\text{O}_{18}$) is a chemically complex and highly compositionally variable gem-forming mineral found in a variety of geologic settings worldwide (see Fig. 12.5). The beryl structure typically consists of hexagonal rings comprised of six SiO_4^{2-} tetrahedra that are stacked parallel to the c-crystallographic axis to produce a mineral structure with hollow central channels, which allows for the substitution of multiple ions of different size [4]. Consequently, coupled ionic substitution is common, with Li^+ regularly substituting for Be^{2+} , Mg^{2+} , Fe^{2+} , Fe^{3+} ,

Mn^{2+} , Cr^{3+} , V^{3+} , and Ti^{4+} substituting for Al^{3+} ; and Be^{2+} or Al^{3+} substituting for Si^{4+} . Additionally, alkali cations (Na^+ , K^+ , Cs^+ , and Rb^+) that are not usually considered as part of beryl's chemical formula can be incorporated. Pure beryl is colorless, but can be strongly colored due to the diversity of trace elements that can enter the mineral structure to yield a variety of colored gemstones.

McMillan et al. [76] demonstrated that single-pulse, broadband LIBS spectra collected over the spectral range of 200–960 nm for 96 beryls from 16 countries and 10 US states could be used to determine the provenance of the samples with a high degree of success. The laser pulse energy, time delay, and crystallographic orientation were optimized to minimize the coefficient of variance for multiple analyses of an individual specimen. Figure 12.8 illustrates how examples of emeralds from seven different countries have recognizably different LIBS spectra. In a subsequent study, 39 beryl specimens from 11 pegmatite mines in New Hampshire, Connecticut, and Maine (USA) were analyzed to assess the potential of PCA of LIBS spectra to determine specimen provenance [50]. Beryl samples from the three different beryl-bearing zones in a New Hampshire pegmatite were recognized. However, the compositional variation within this single mine was found to be comparable to that for beryls from all other locations, a feature attributed to its unusual geological complexity.

12.3.3.2 Corundum

Trace amounts of metals in corundum, an aluminum oxide ($\alpha\text{-Al}_2\text{O}_3$) mineral that is colorless in its pure form, are responsible for the blue color typically associated with sapphires (iron and titanium) and the red color of rubies (chromium). Thermal processing of corundum and other minerals has been used for centuries to enhance color and increase the value of lower-grade gemstones. This approach is normally considered a 'traditional enhancement', it being an acceleration of the natural processes that operate in the earth to form gemstones. However, artificial treatments, such as beryllium diffusion of corundum, have been used to create gem-quality stones with hues that mimic natural materials. Such enhanced corundum is virtually indistinguishable from substantially more expensive natural gemstones without the use of an elemental analysis technique capable of detecting Be in the low ppm range.

While LA-ICP-MS and SIMS have been successfully utilized to analyze for the presence of Be-enhanced corundum and to determine provenance of natural gemstones [49], the instrumentation is expensive and not readily available in most gemological laboratories. In order to find a more economical substitute, researchers at the Schweizerisches Gemmologisches Institut (Swiss Gemological Institute) used LIBS to detect Be-diffused sapphire and ruby [104, 105]. While not as sensitive as LA-ICP-MS, LIBS was able to detect Be concentrations down to a few ppms, and this was sufficient to identify enhanced gemstones. Damage to the sample consisted of a small crater ($\sim 100\text{ }\mu\text{m}$) but this could be kept at a minimum by careful choice of experimental parameters and precise focusing.

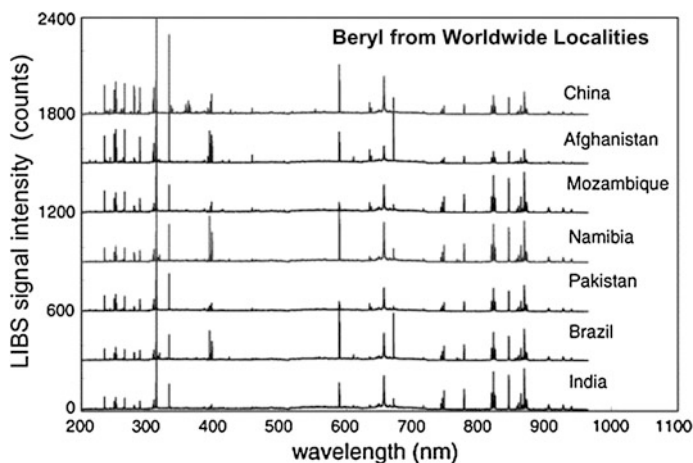


Fig. 12.8 Broadband LIBS spectra for emerald specimens from seven countries (China, Afghanistan, Mozambique, Namibia, Pakistan, Brazil and India) showing readily discernible differences in the 250–400 and 600–700 nm regions [99]

12.3.3.3 Garnet

Garnets are silicates known to have a widely varying major element composition that can be represented by the general formula $X_3Y_2(SiO_4)_3$, where X and Y respectively refer to cation sites of 8-fold and 6-fold coordination with the X site hosting large divalent cations (e.g., Ca^{2+} , Mg^{2+} , Fe^{2+} , Mn^{2+}) and the Y site occupied by smaller trivalent cations (e.g., Fe^{3+} , Cr^{2+} , Al^{3+}) [4]. Garnets very rarely, if ever, occur naturally as pure end-member compositions, so that names are assigned based on the dominant molecular type: andradite $[Ca_3Fe_2(SiO_4)_3]$, grossular $[Ca_3Al_2(SiO_4)_3]$, uvarovite $[Ca_3Cr_2(SiO_4)_3]$, almandine $[Fe_3Al_2(SiO_4)_3]$, pyrope $[Mg_3Al_2(SiO_4)_3]$, and spessartine $[Mn_3Al_2(SiO_4)_3]$. Six other minor species of garnet are known to occur in nature, but are uncommon. Typically, garnets crystallize as rhombic dodecahedrons, trapezohedrons, or a mixture of these two crystal forms. Garnets can range in color from colorless to red, pink, orange, yellow, green, blue, purple or black. While the identity of a garnet species can be inferred from color, refractive index, and magnetic susceptibility measurements [106], elemental analysis is required for positive identification.

Alvey et al. [53] collected broadband LIBS spectra for a suite of 157 garnets from 92 locations worldwide. The data demonstrated that LIBS could be used to discriminate garnets of different composition and has the potential to discern geographic origin. In Fig. 12.9, spectral differences are clearly seen in the broadband LIBS spectra of the six common garnet types. It was straightforward to discern between near end-member specimens based on the presence of lines corresponding to Al, Ca, Cr, Fe, Mg, and Mn. However, since most garnets are found as mixtures of more than one type in solid solution it was found that

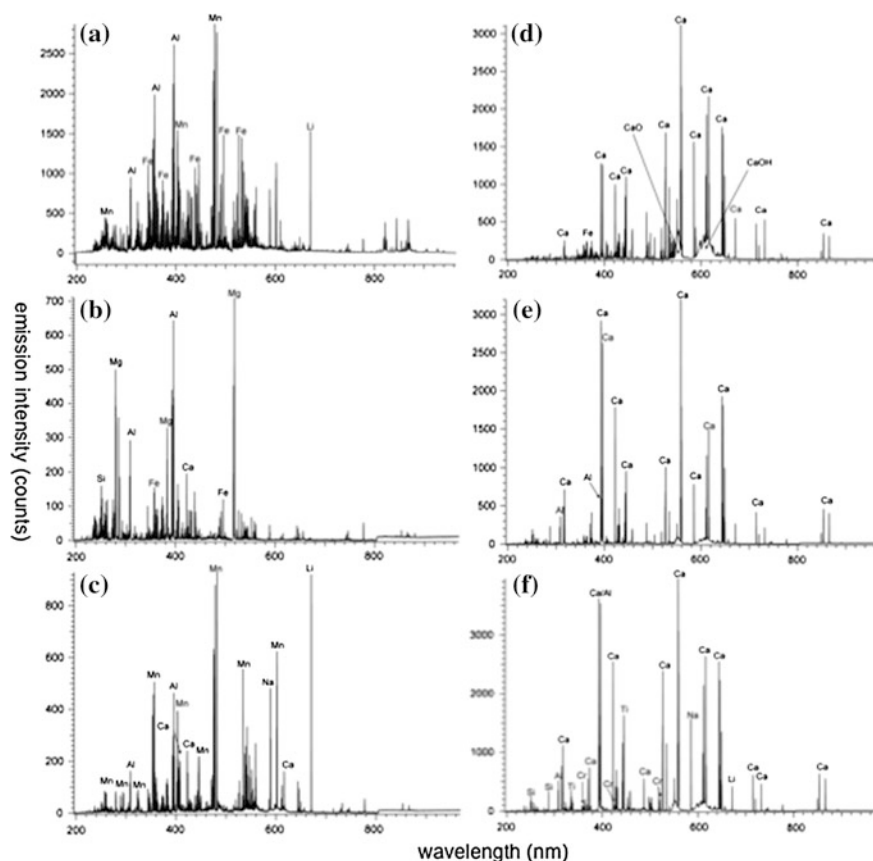


Fig. 12.9 Spectral differences are clearly seen in the broadband LIBS spectra of six common garnet compositional types: **a** almandine [$\text{Fe}_3\text{Al}_2(\text{SiO}_4)_3$], **b** pyrope [$\text{Mg}_3\text{Al}_2(\text{SiO}_4)_3$], **c** spessartine [$\text{Mn}_3\text{Al}_2(\text{SiO}_4)_3$], **d** andradite [$\text{Ca}_3\text{Fe}_2(\text{SiO}_4)_3$], **e** grossular [$\text{Ca}_3\text{Al}_2(\text{SiO}_4)_3$], and **f** uvarovite [$\text{Ca}_3\text{Cr}_2(\text{SiO}_4)_3$]

chemometric approaches were preferable for classifying specimens. PLSDA with LOSO cross-validation using 25 laser pulses for each of the samples produced a nearly 95 % correct classification rate based on garnet type. A similar analysis was able to correctly identify the major garnet group—either the Ca *ugrandite* group (uvarovite, grossular, and andradite) or Al *pyrope* group (pyrope, almandine, spessartine) of a sample 98 % of the time.

The task of matching a sample with its correct geographic origin is more challenging and requires a large sample suite to ensure the characteristic ‘spectral fingerprint’ is properly captured. For the garnet study, PLSDA on the LIBS spectra obtained from a subset of 87 garnets produced only a 55 % correct classification rate, with localities represented by the greater number of samples furnishing correspondingly better discrimination. Using *variable importance in projection* (VIP)

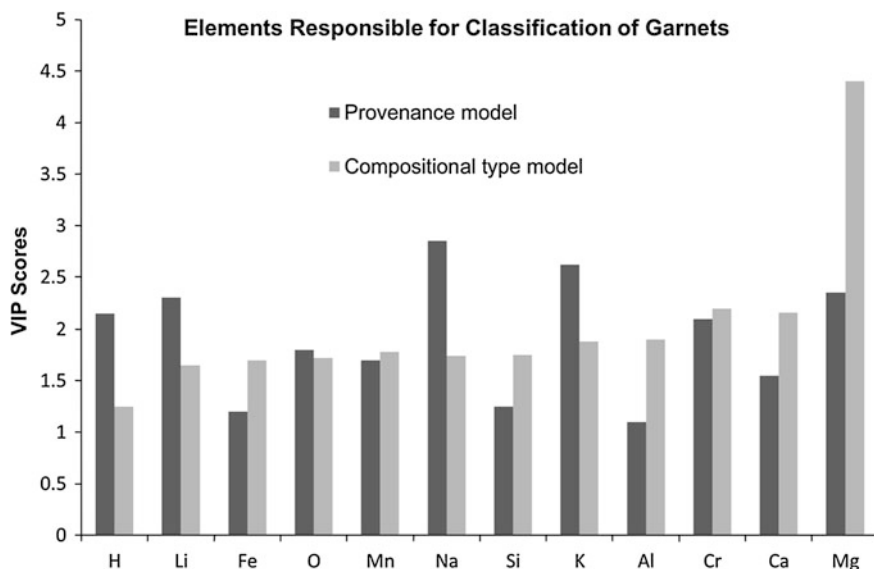


Fig. 12.10 Variable importance in projection (*VIP*) scores plot derived from the PLSDA model showing which elements are responsible for classification of garnets from worldwide locations according to the provenance (*dark bars*) and compositional type (*light bars*) (modified from [86])

scores it is possible to discern which wavelengths, and therefore which elements, have greatest importance in the classification algorithm (Fig. 12.10). It was found that the wavelengths most useful for garnet composition classification (i.e. those with the highest *VIP* scores) corresponded to the principal chemical species that differentiate garnet types (Ca, Mg, Al, Fe, Mn, and Cr), whereas the wavelengths of minor impurities (H, Li, Na, and K) were responsible for discrimination based on provenance [53]. This highlights the importance of acquiring a large sample library with many specimens from each locality of interest.

12.3.4 Rocks of Volcanic Origin

There are two applications that make LIBS an attractive analytical technique for volcanologists. The first is the correlation of volcanic strata, particularly in terrains that have been disrupted by faulting and dissected by erosion. The second is for identifying the range of chemical variation within a sequence of lavas, so as to permit efficient sampling of the sequence. There is also strong interest in the archaeological community in being able to determine the provenance of volcanic rocks that have been used for the manufacture of tools by paleo-people.

To test the first application, a suite of 23 samples of volcanic rocks (i.e. lavas, tuffs, tephra) from seven locations in the Andes (N. Chile), Kamchatka, Antarctica

(Mt. Melbourne and Ferrar), and Panama (Chagres, Younger Arc, and Soñá) was analyzed with a commercial LIBS system with broadband detection from ($\sim 200\text{--}965\text{ nm}$) using five cleaning shots followed by 25 laser pulses in a single location. The representative spectra shown in Fig. 12.11 illustrate the visible difference between samples. Five randomly selected spectra were reserved for the test set and the remaining spectra were used to build a PLSDA model. The result for the Panama-Chagres samples is shown in Fig. 12.12 using a model and test sample index chart. In this type of representation (an alternative to the confusion matrix), the robustness of the PLSDA model can easily be visualized as all 40 of the Chagres spectra used to develop the algorithm and the 10 spectra sequestered for testing are much more closely associated with each other than with any of the other sample classes. The PLSDA VIP class scores show that this discrimination is based principally upon varying amounts of Li, Na, Mg, Al, K, Ca, and Ti.

A related study utilized a suite of volcanic rocks from around the world that were associated with historic volcanic events ranging in time from the eruption of Vesuvius that destroyed Pompeii in 79 AD to a recent eruption in the Galapagos Islands [108]. The sample suite contained 13 pristine volcanic rocks that had not been subjected to any secondary alteration that might have affected their chemical composition. The silica content covered the natural compositional range of volcanic rocks ($\text{SiO}_2\text{ \%} \sim 48\text{--}75\text{ wt\%}$). The rocks were analyzed with a commercial LIBS system with broadband detection ($\sim 385\text{--}620\text{ nm}$) at moderate resolution ($0.2\text{--}0.3\text{ nm}$) using 25 cleaning shots followed by 100 laser pulses in each location of a 2×3 grid. The data was then processed through a PLSDA classifier that used 20 components to build a robust model for analysis. The results summarized in Table 12.3 show that 92 % of the samples could be correlated with the correct origin. The single misclassification, a piece of tephra from the Galapagos, was probably due to the poor coupling of the laser with the “airy” sample, which suggests that additional preprocessing may be necessary when analyzing this type of volcanic rock. These results could potentially be improved by performing the analysis with a broader spectral range and at greater resolution in order to better capture the elemental variability of the volcanic rocks. Increasing the number of PLSDA components would probably not improve the percent correlation, but may have led to over-training the model.

12.3.4.1 Obsidian

Obsidian is a natural, felsic glass of volcanic origin that is rich in silicon dioxide (SiO_2) and exhibits a conchoidal fracture. Obsidian is formed on either the margins of lava domes or as extrusive lava flows over an area of high silicic rhyolite volcanism, in which it then cools very rapidly leaving it without a crystal structure. Obsidian can be found all over the world, with a large number of sources in the United States, particularly in California and other western states. A sample of obsidian typically contains over 70 % SiO_2 and incorporates significant amounts of Al, Ca, Fe, Mg, Mn, K, Na, and Ti along with trace amounts of transition metal,

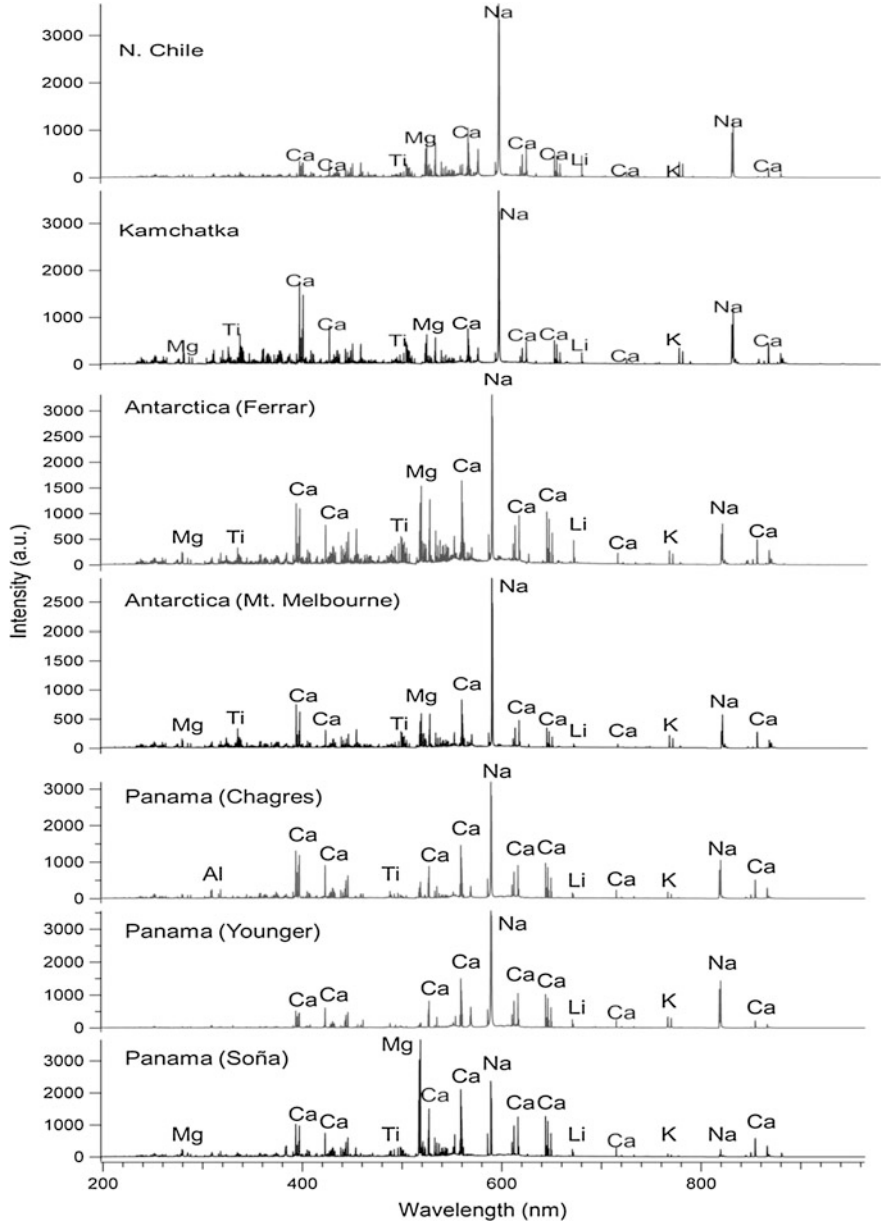


Fig. 12.11 Representative broadband LIBS spectra of volcanic samples from seven locations in the Andes (N. Chile), Kamchatka, Antarctica (Mt. Melbourne and Ferrar), and Panama (Chagres, Younger Arc, and Soña) with major emission lines labeled to show how the chemical composition varies with geographic origin [107]

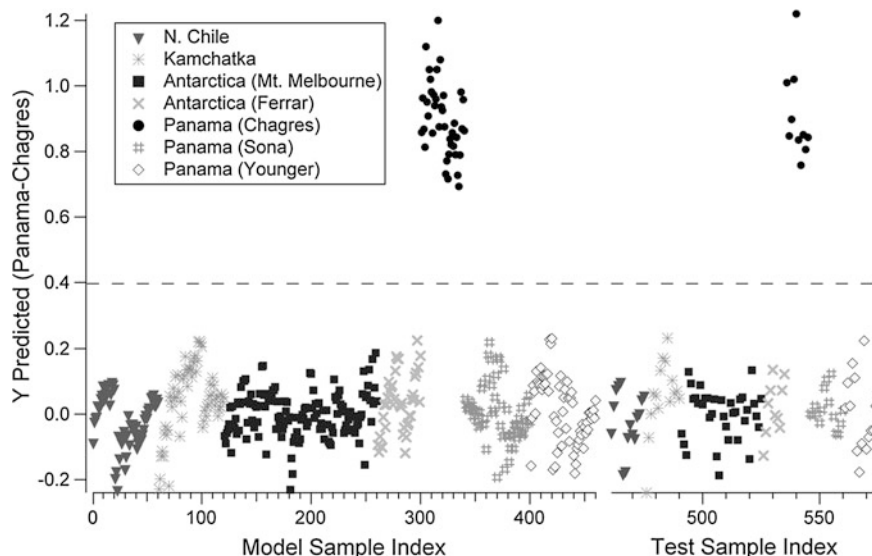


Fig. 12.12 Visualization of the PLSDA classification result for the Panama—Chagres samples in which the prediction value for the model class is plotted against the model and test sample index. The 40 Chagres spectra used when building the PLSDA model as well as the 10 Chagres test spectra fall well above the threshold shown illustrating the quality of the match with the assigned model class [107]

lanthanide, and actinide cations that vary from one source to another as illustrated in Table 12.4 [58]. Variation in the abundance of these minor and trace elements has been used as the basis for establishing a geochemical fingerprint for the purpose of distinguishing obsidian from different local sources [48, 109]. However, due to the previously stated drawbacks of the analytical techniques that have been used for such analysis (e.g., XRF, INAA, and ICP-MS), there is significant interest in applying LIBS to obsidian origin studies (see Fig. 12.2 for examples of LIBS spectra of obsidian).

In a study that has important implications for the use of LIBS as a tool for archeological applications, Remus et al. [98] used a commercial LIBS instrument equipped with a Nd:YAG 1,064 nm laser operating at ~ 70 mJ to acquire 100 single-pulse, broadband spectra (~ 200 – 980 nm) for 31 obsidian samples from multiple locations in the Coso Volcanic Field (CVF) in California and additional sites in eastern California and western Nevada. A total of 185 emission lines for 18 species (corresponding to Al, Si, O, Mg, Fe, Mn, Ca, Na, H, K, Ti, Li, N, Sr, Ba, Er, Be, and AlO) were identified, background corrected, normalized to the sum of the line intensities, and utilized to generate 153 emission line ratios. Individual summed line intensities and ratios from 3,100 spectra were used to build and test multiple PLSDA models. It was found that obsidian from the five distinct California-Nevada source areas could easily be distinguished from one another.

Table 12.3 Classification confusion matrix for the PLSDA analysis of 13 historical volcanic rock samples (with the year of the volcanic event shown in parentheses, when known) using 600 LIBS spectra per sample and 20 latent variables to produce 13 model classes. All but one of the samples (tephra from Sierra Negra) are correctly classified according to geographic provenance when a “most votes” approach is employed [108]

| Sample # | Test Samples | Model Classes | | | | | | | | | | | | |
|----------|---------------------------------------|---------------|-----|-----|-----|-----|-----|----|-----|-----|-----|-----|-----|-----|
| | | 1 | 2 | 3 | 4 | 5 | 6 | 7 | 8 | 9 | 10 | 11 | 12 | 13 |
| 1 | <i>Mount St. Helens, USA (1980)</i> | 599 | 0 | 0 | 0 | 0 | 0 | 0 | 1 | 3 | 0 | 0 | 0 | 0 |
| 2 | <i>Mt. Erebus, Antarctica</i> | 0 | 599 | 0 | 0 | 0 | 0 | 0 | 0 | 0 | 0 | 0 | 1 | 0 |
| 3 | <i>Vesuvius, Italy (79 AD)</i> | 0 | 0 | 533 | 0 | 0 | 0 | 0 | 0 | 0 | 0 | 0 | 0 | 67 |
| 4 | <i>Vesuvius, Italy (1944)</i> | 0 | 0 | 0 | 598 | 0 | 0 | 0 | 0 | 0 | 0 | 1 | 1 | 0 |
| 5 | <i>Stromboli, Italy (1990)</i> | 0 | 0 | 0 | 0 | 483 | 1 | 62 | 0 | 8 | 7 | 0 | 1 | 38 |
| 6 | <i>Mauna Ulu, USA (1975)</i> | 0 | 0 | 0 | 0 | 0 | 600 | 0 | 0 | 0 | 0 | 0 | 0 | 0 |
| 7 | <i>Sierra Negra, Galapagos (2005)</i> | 0 | 0 | 0 | 0 | 0 | 0 | 22 | 0 | 0 | 0 | 0 | 0 | 578 |
| 8 | <i>Lipari, Italy (~1400 AD)</i> | 0 | 0 | 0 | 0 | 0 | 0 | 0 | 600 | 0 | 0 | 0 | 0 | 0 |
| 9 | <i>Paricutin, Mexico (1952)</i> | 0 | 0 | 0 | 0 | 0 | 0 | 0 | 0 | 595 | 2 | 0 | 3 | 0 |
| 10 | <i>Mayon, Philippines (1984)</i> | 0 | 0 | 0 | 0 | 24 | 0 | 3 | 0 | 0 | 505 | 1 | 3 | 64 |
| 11 | <i>Arenal, Costa Rica (1968)</i> | 0 | 0 | 0 | 0 | 5 | 0 | 72 | 3 | 3 | 4 | 343 | 49 | 44 |
| 12 | <i>Santorini, Greece</i> | 0 | 0 | 0 | 0 | 0 | 0 | 0 | 0 | 0 | 0 | 1 | 599 | 0 |
| 13 | <i>Krakatoa, Indian Ocean (1883)</i> | 0 | 0 | 0 | 0 | 0 | 0 | 0 | 0 | 0 | 0 | 0 | 0 | 600 |

However, correct classification of samples from eight sub-source locations within the CVF was more problematic. This could be attributable to the fact that LIBS is not sufficiently sensitive to detect differences in trace elements known to be present in the sub-ppm range. When the individual CVF locations were regrouped into four subsources, according to the timing of the eruptive events that created them, then LIBS was able to correctly match 24 out of 27 (89 %) samples. In this case, the results of chemometric analysis of LIBS data was in agreement with the subsample groupings suggested by geochemical evidence derived from other analytical techniques (e.g. LA-ICP-MS).

In order to address questions about the efficacy of various chemometric processing approaches, 50 spectra from two wavelength regions (218–474 and

Table 12.4 A comparison of seven obsidian samples from the Coso Volcanic Field, California (USA) illustrating major (weight % level) and trace element (ppm level) variation (modified from Remus et al. [98])

| | | Sample # | | | | | | |
|------------------------------------|-----------------------|----------|-------|------|-------|-------|-------|-------|
| Chemical Species | | 1 | 2 | 3 | 4 | 5 | 6 | 7 |
| <i>SiO₂</i> | <i>Weight percent</i> | 74.5 | 74.7 | 76.5 | 75.8 | 76.5 | 76.7 | 77.9 |
| <i>Al₂O₃</i> | | 12.62 | 12.29 | 12.2 | 12.15 | 12.57 | 12.45 | 12.54 |
| <i>K₂O</i> | | 4.6 | 4.25 | 4.53 | 4.3 | 4.58 | 4.61 | 4.37 |
| <i>Na₂O</i> | | 4.15 | 4.38 | 4.12 | 4.12 | 4.32 | 4.34 | 4.32 |
| <i>Fe₂O₃</i> | | 0.69 | 0.47 | 0.38 | 0.34 | 0.31 | 0.4 | 0.43 |
| <i>FeO</i> | | 0.31 | 0.55 | 0.45 | 0.46 | 0.65 | 0.63 | 0.5 |
| <i>CaO</i> | | 0.4 | 0.51 | 0.37 | 0.5 | 0.42 | 0.41 | 0.38 |
| <i>TiO₂</i> | | 0.05 | 0.07 | 0.04 | 0.05 | 0.07 | 0.09 | 0.04 |
| <i>MgO</i> | | 0.05 | 0.01 | 0.01 | 0.06 | 0.02 | 0.02 | 0.03 |
| <i>MnO</i> | | 0.03 | 0.02 | 0.02 | 0.02 | 0.02 | 0.02 | 0.02 |
| <i>Rb</i> | <i>ppm</i> | 425 | 305 | 340 | 245 | 195 | 210 | 230 |
| <i>Zr</i> | | 100 | 100 | 95 | 95 | 140 | 135 | 95 |
| <i>Nb</i> | | 90 | 100 | 74 | 50 | 52 | 49 | 50 |
| <i>Y</i> | | 74 | 74 | 73 | 58 | 47 | 47 | 62 |
| <i>Zn</i> | | 66 | 59 | 59 | 42 | 49 | 45 | 45 |
| <i>Th</i> | | 42 | 35 | 35 | 28 | 26 | 25 | 29 |
| <i>Pb</i> | | 37 | 35 | 33 | 27 | 23 | 26 | 29 |
| <i>La</i> | | 13 | 17 | 19 | 19 | 44 | 41 | 17 |
| <i>U</i> | | 14 | 14 | 12 | 10 | 8 | 8 | 13 |

568–804 nm) for each of 170 samples were collected to create an obsidian source library [54]. The data were processed using PLSDA with LOSO cross validation. Materials from the six major California obsidian source areas in this study could be effectively discriminated with high rates of sample-level classification. In particular, it was found that ~90 % classification success was possible using either wavelength region. Discrimination performance was essentially the same for single pulse spectra compared to ten-shot averages. Fusion of the data sets for the two spectral regions gave slightly better performance, with ‘decision-level’ fusion (i.e. the two sets of data were processed separately with different PLSDA algorithms, class labels were estimated, and then a final label estimate was generated) slightly outperforming ‘feature-level’ fusion (i.e. the spectral data were stitched together to form amalgamated spectra).

Hrdlička et al. [61] used a double pulse LIBS system to analyze 12 obsidian glass samples consisting of natural material and artifacts obtained from sites in the Czech Republic, Slovakia, Germany, Hungary, Greece, Turkey and Ukraine. A low energy pulse from a 266 nm laser (10 mJ) was followed by an orthogonal 1,064 nm laser pulse (100 mJ) to produce strong emission lines for Si, Mg, Ca, Na, Al, Fe, Ti, Sr, Ba, and K. This experimental set-up produced nearly undetectable damage to the samples. Though the double pulse method is typically very sensitive

the anticipated rare earth elements could not be detected. A variety of multidimensional statistical approaches were used to successfully match up artifacts with their place of origin.

Archeological Applications

Archaeological materials can provide important information about the timing, strength, and longevity of prehistoric trading patterns. Multi-element chemical analysis has become a common means for attributing the provenance of different kinds of artifacts (e.g., tools, pottery, and ornamental materials) [58]. Because it fractures conchoidally, obsidian was commonly used by native peoples for tools and was exchanged extensively within North America. The CVF in California, for example, contains a large number of high-silica rhyolite domes, many of which contain obsidian glass that was quarried for tools by the indigenous population for more than 12,000 years. Coso-Type obsidian artifacts are found throughout the southwestern United States.

A preliminary study involving 12 obsidian artifacts was carried out as part of an ongoing effort to develop a comprehensive obsidian source library suitable for archeological purposes [110]. Forty single-shot LIBS spectra were collected for each spot on a 2×2 grid over two spectral windows (218–474 and 568–804 nm) for a suite of 299 obsidian samples from 10 California/Nevada obsidian localities, most of which had multiple sub-sources. After removal of 15 cleaning shots per grid location, the resulting 100 spectra per sample formed the input for PLSDA models. As observed in previous studies, materials from the six major California obsidian source areas could be discriminated effectively but identification of subsources was more challenging. A subset of these data for three California locations (Rose Spring in the CVF, Saline Range, and Bodie Hills) was used to train a PLSDA algorithm. Spectra obtained from a dozen artifacts believed to originate from these three areas were used to evaluate the performance of the model. It was possible to match up the artifacts with the putative sources with a high degree of success using both wavelength regions as shown in Table 12.5.

12.3.5 Conflict Minerals

Geological materials illicitly mined or sold in conditions of armed conflict and human rights abuse are known as *conflict minerals*. So-called ‘blood diamonds’ are most familiar to the public but other gemstones as well as high-value commercial ores also fall into this category. The sale of conflict diamonds from western and central Africa has been one means of funding rebel groups in this region since the 1970s. Although the focus of the mineral exploitation issue by armed groups usually centers on Africa, other areas prone to ongoing strife are also affected. International efforts, such as the Kimberly Process for diamonds, have been

Table 12.5 PLSDA classification results for an obsidian artifact attribution study showing the percentage of spectra from each of the 12 artifacts that were assigned to a previously identified obsidian source for two wavelength regions: (A) 218–474 nm and (B) 568–804 nm [110]

| | Test sample | Model class | | |
|---|--------------------------|-------------------|-------------|--------------|
| | | Rose spring (CVF) | Bodie hills | Saline range |
| A | <i>Rose spring (CVF)</i> | 100 | 0 | 0 |
| | <i>Bodie hills</i> | 3 | 97 | 0 |
| | <i>Saline range</i> | 6 | 2 | 83 |
| B | <i>Rose spring (CVF)</i> | 99 | 0 | 0 |
| | <i>Bodie hills</i> | 4 | 96 | 0 |
| | <i>Saline range</i> | 2 | 11 | 84 |

developed in an attempt to stem the illegal trade in conflict minerals. More recently, the Dodd-Frank Wall Street Reform and Consumer Protection Act of 2010 requires U.S. companies to report annually to the Securities and Exchange Commission (SEC) whether their products contain gold, tantalum, tin, or tungsten obtained from the Democratic Republic of the Congo (DRC) or adjacent countries. In the absence of verifiable means for establishing the origin of raw materials manufacturers and consumers have resorted to region-wide boycotts. Development of the means to identify the provenance of ‘conflict minerals’ therefore has taken on increased urgency as part of an effort to minimize the negative impact of such actions on legitimate mining operations in non-conflict areas.

12.3.5.1 Columbite-Tantalite (Coltan)

Niobium and tantalum are rare metals whose natural occurrence is primarily in the complex oxide minerals columbite and tantalite, which form a solid-solution series having the general composition $[\text{Fe}, \text{Mn}][\text{Nb}, \text{Ta}]_2\text{O}_6$. Due to the commercial importance of niobium (used to make hardened steel alloys) and tantalum (essential for the production of electronic components used in consumer electronics) these minerals are very valuable. The export of columbite-tantalite ore, which is known as *coltan*, from the DRC and neighboring Great Lakes region of central Africa countries is one of several potential revenue streams for the combatants engaged in conflict over politics, land and tribal issues.

Laboratory-based techniques, which are principally dependent on quantitative elemental and isotope analysis utilizing scanning electron microscopy (SEM) and LA-ICP-MS, have been successfully developed to match a sample of columbite-tantalite obtained from a given mine site with samples from the same mine previously cataloged in a database [111–113]. However, the instrumentation is expensive and non-portable and requires time-consuming sample preparation. Consequently, the approach cannot be used in the field. On the other hand, a LIBS-based system for identifying the origin of minerals would not require sample preparation, would give answers quickly, and could be designed for field use.

A pilot study to explore the application of LIBS-based geochemical fingerprinting for coltan provenance determination was carried out using 14 samples from three locations in North America [22]. After cleaning the surface of the bulk mineral with 15 laser pulses at each location on a 2×2 grid, a total of 100 emission spectra were collected and used to create a PLSDA model with LOO cross-validation. A $>90\%$ correct classification rate was achieved and it was found that the PLSDA loadings (aggregated across all three classes) with the largest magnitude corresponded to emission lines of anticipated major and trace elements of the columbite group minerals (e.g., Fe, Mn, Zr).

In a follow-up study, a more geographically diverse set of 57 columbite-tantalite samples from 28 worldwide locations were analyzed using a similar protocol [23]. The spectral range from 250 to 490 nm was again chosen to include many of the intense emission lines for the major elements (Ta, Nb, Fe, Mn) and the significant trace elements (e.g., W, Ti, Zr, Sn, U, Sb, Ca, Zn, Pb, Y, Mg, and Sc) known to commonly substitute in the columbite-tantalite crystal structure. Multivariate statistical signal processing (PLSDA with 15-fold cross-validation) resulted in 98 % correct sample-level classification, when a “majority votes” approach was used. The PLSDA loadings data suggest that low concentrations of rare-earth elements, such as Y, Gd, Yb and Lu, may be a contributing factor for the high level of sample discrimination. Preliminary studies with a portable LIBS prototype were conducted with a small yet geographically diverse subset of this coltan sample suite [114]. Chemometric analysis using PLSDA gave excellent classification results but much additional work is required to transition from laboratory-based instrumentation to LIBS systems that can be used in the field [77].

Ultimately, the purpose of these studies is to discover if a LIBS-derived geochemical fingerprint of coltan can be used to distinguish between conflict and non-conflict (or legal and illegal) sources at acceptable confidence levels. Preliminary results from the analysis of a suite of 32 columbite-tantalite samples from several central African countries (DRC, Mozambique, Namibia, Rwanda, and Zimbabwe) are encouraging [115]. Interrogation of the samples, which were embedded in resin and polished for a previous study, was accomplished using 40 single pulses from a 1,064 nm Nd:YAG laser at each location of a 2×2 grid. A typical spectrometer gate delay of 2 μ s and a gate width of 3 μ s were employed to give a total of 100 spectra per sample after removal of cleaning shots. For this experiment the wavelength range of 240–490 nm was chosen. Chemometric processing of the 3,200 spectra using PLSDA with random folds cross-validation gave over a 93 % correct classification rate. A 3-D plot of the first three principal components (Fig. 12.13) graphically illustrates the significant clustering of the coltan samples. While this suggests that samples from different locations in central Africa have sufficiently dissimilar spectral fingerprints to allow for discrimination, further work is required. For example, no attempt was made in this study to ensure that the laser was ablating material corresponding to columbite-tantalite and not the associated matrix minerals. It was also noted that a country-level PLSDA classification task resulted in approximately one-third of the samples being matched

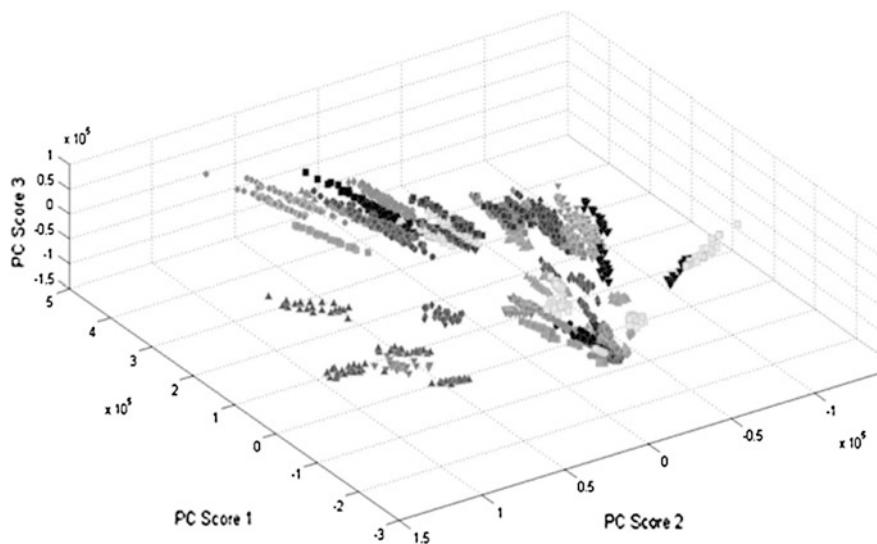


Fig. 12.13 3-D principal component analysis plot created using 3,200 LIBS spectra for 32 conflict mineral samples from central African countries, including conflict and non-conflict sources. The samples were each assigned to individual model classes. The sample suite was provided courtesy of the Bundesanstalt für Geowissenschaften und Rohstoffe (Federal Institute for Geosciences and Natural Resources) [115]

back to the incorrect country. Since political boundaries are not formulated on the basis of geology, these findings were not unexpected but they do highlight the need for caution when applying this approach.

12.3.5.2 Cassiterite

Cassiterite (SnO_2) is the chief ore used in the industrial production of tin. The tin extracted from this ore is used primarily for soldering in the electronics industry. The worldwide technology “boom” of the last decade is one factor that has pushed the cost of this metal from a relatively stable average price per metric ton of approximately 5,000 USD (1994–2003), through price spikes of over 32,000 USD (early 2011), to the current cost of about 20,000 USD (2013) [116]. The increase in demand and relatively large supply of cassiterite in the underdeveloped DRC and surrounding countries has contributed to the growth of illicit trading of this ‘conflict’ commodity by armed groups.

In order to determine if the geographic origin of cassiterite could be identified using LIBS a total of 38 ore concentrate samples from South America and Southeast Asia were analyzed at three different wavelength regions (220–440, 460–700, and 680–910 nm) with a spectrometer having 0.2–0.3 nm resolution [117]. The data from the three data sets were stitched together after removal of redundant wavelengths to create an artificial broadband spectrum. The sampling

Table 12.6 PLSDA confusion matrix generated using 80 components and 10-fold cross-validation for the analysis of 38 cassiterite samples classified by country of origin

| Test samples (# of Examples) | Model classes | | | | | |
|------------------------------|---------------|------|----------|-----------|--------|----------|
| | Bolivia | Peru | Thailand | Indonesia | Brazil | Malaysia |
| <i>Bolivia</i> (19) | 83 % | 0 | 1 % | 2 % | 3 % | 6 % |
| <i>Peru</i> (9) | 3 % | 94 % | 1 % | 0 % | 0 % | 2 % |
| <i>Thailand</i> (4) | 0 | 0 | 99 % | 0 | 0 | 1 % |
| <i>Indonesia</i> (4) | 0 | 0 | 1 % | 99 % | 0 | 0 |
| <i>Brazil</i> (1) | 0 | 0 | 1 % | 0 % | 99 % | 0 |
| <i>Malaysia</i> (1) | 1 % | 0 | 0 % | 0 % | 0 % | 99 % |

protocol involved using four laser pulses at each location of a 5×5 grid to give 100 spectra for each sample. The samples were in either powdered or granular form and thus needed to be interrogated at low laser power (~ 9 mJ) in order to reduce the amount of material scattered into the air by the ablation process. The data was passed through a PLSDA classifier that employed 120 components and 10-fold cross-validation to build a robust model that provided an overall correct sample-level classification rate of 97 %. A smaller number of PLSDA components gave correspondingly lower, but still acceptable, classification rates. When the sample suite was grouped according to the eleven locations from which the ore concentrate was mined the PLSDA model gave a correct classification rate of 87 % (Table 12.2). Contrary to the coltan example cited earlier, when the 38 samples were consolidated into six different classes based on the country the ore was extracted from the resulting confusion matrix still showed good results (Table 12.6).

While these results suggest that coltan and cassiterite specimens can be discriminated from one another on the basis of their spectral fingerprints additional work is required to establish LIBS as an effective component of the solution for the conflict minerals issue [118]. In particular, a large spectral library, comprised of multiple samples gathered from numerous mine sites in central Africa over a period of time, must be created. By adequately sampling inter- and intra-source compositional and temporal heterogeneity the number of misclassifications can potentially be reduced to known and acceptable levels, though mixed samples may still pose a problem. In order to use the LIBS approach in the field (e.g., at the point of collection or sale of ore concentrate, before material from multiple sources has been comingled and the geochemical fingerprint obscured or entirely lost) the question of the effect of matrix minerals also has to be addressed. The spectral fingerprint derived from analysis of ore concentrate reflects the amount of matrix minerals still present in the sample after preliminary processing. If processing patterns shift over time this could affect the LIBS spectra even though the geochemistry of the mineral vein itself is unchanged. In the absence of any sample preparation to ensure that only grains of the conflict mineral of interest are being interrogated by the laser, a routine for preprocessing LIBS spectra using spectral sorting algorithms needs to be developed. LIBS-based provenance classification may find its best application as a presumptive field screening tool to complement the existing confirmatory techniques available in the laboratory [119].

12.3.6 Other Geomaterials

Since this volume contains sections dedicated to LIBS analysis of soil ([Chap. 5](#)—“Elemental analysis of soils by means of LIBS”) and coal ([Chap. 13](#)—“LIBS analysis for coal”), only a brief mention will be made of the application of geochemical fingerprinting for these materials in this chapter.

The use of LIBS for identification of soil provenance is of significant interest for agricultural, environmental, and forensic applications. LIBS has been used to identify and map Pb levels in contaminated soil at the Sierra Army Depot using both laboratory-based and portable instrumentation [63]. A study of 149 Brazilian soil samples demonstrated that high levels of discrimination could be obtained along with reduced computational workload by using wavelet domain data compression prior to chemometric processing [120]. LIBS was also successfully applied to forensic analysis of bulk soil samples and geographic site characterization from three locations in Dade County, FL, with discrimination rates comparable to those obtained with LA-ICP-MS [121]. LIBS has been principally applied to the fingerprinting of coal for inline monitoring of ash content at coal-fired power plants [122, 123].

12.4 Future Development of LIBS for Geochemical Fingerprinting

The emission spectra generated in laser-induced breakdown spectroscopy can serve as the chemical signature of materials for the purpose of geochemical fingerprinting. The relative advantages and disadvantages of using LIBS for provenance determination have been discussed. The chemometric processes used to correlate LIBS data with geographic point of origin were also described. Though this approach has been applied to, and its efficacy demonstrated for, a substantial variety of geological materials, there is still much work to be done in this area.

In order to more fully establish the validity of and realize the full potential of the LIBS technique for geochemical fingerprinting researchers need to analyze even larger, more comprehensive sample suites that contain materials with known, unambiguous provenance. The number of samples should be sufficient to allow for robust chemometric analysis (e.g., PLSDA using LOSO cross-validation) and to adequately represent the range of chemical variety associated with the specific class of geomaterials being analyzed. For example, the reliability of LIBS as a tool to distinguish ore originating from conflict and non-conflict regions (or from legal or illegal mining operations) is a function of how many mine locations are sampled—interrogating samples from more potential sources will provide a more reliable answer when trying to establish provenance.

Likewise, it is important to verify what elements are responsible for discrimination between samples to ensure that the results are reasonable in a geological

sense. LIBS data could be correlated with other analytical techniques such as EMP or LA-ICP-MS to confirm the source of discrimination. This is especially important when dealing with materials such as ore concentrates or rocks that contain mixtures of mineral species. Qualitative analysis of such samples using chemometric approaches will reflect not only the intrinsic chemical composition of a particular mineral of interest but also the matrix materials invariably associated with it. Ideally, it should be possible to distinguish between the geochemical fingerprint of a specific mineral, which may have minimal variation within the same geologic deposit, and an orebody whose composition can be affected by alterations in mining protocols. Additional work is required along these lines to explore chemometric methodologies to deal with samples with mixed provenance. In general, the reliability of LIBS-based geochemical fingerprinting would be strengthened if multiple chemometric approaches (e.g., PLSDA, SIMCA, ANN) gave the consistent classification results when applied to the same data set.

In order to advance LIBS as a geochemical fingerprinting technique, it is essential to move the method from the realm of academic investigations carried out by spectroscopists in laboratory settings to field trials that address realistic situations encountered by practitioners such as geologists, archeologists, and professionals in the mining industry. The engineering requirements for ruggedized, portable instruments need to be further developed so that commercial-off-the-shelf (COTS) units become available at a reasonable cost. Perhaps LIBS greatest strength lies in its adaptability as a real-time instrument for use in the field. Other techniques can outperform LIBS in a laboratory setting but they are not amenable for field use. For example, it would be quite advantageous to have a portable LIBS unit that could be used as a reliable screening tool for ore concentrate at an early stage of the commercial chain. Such a system would nicely complement the more accurate and precise laboratory-based analytical protocols as part of a comprehensive process for ascertaining the provenance of minerals obtained from the DRC and surrounding Great Lakes region of central Africa.

LIBS represents a highly useful analytical technique with many features that make it very appealing for geochemical fingerprinting. When combined with chemometric analysis the LIBS method will continue to find many applications in the area of geochemical analysis.

References

1. J. Hoefs, *Eur. J. Mineral.* **22**, 3 (2010)
2. B.S. Kamber, *Appl. Geochem.* **24**, 1074 (2009)
3. B.J. Skinner, P.B. Barton Jr, *Annu. Rev. Earth Planet. Sci.* **1**, 183 (1973)
4. C. Klein, B. Dutrow, *The 23rd Edition of the Manual of Mineral Science* (Wiley, Hoboken, 2008)
5. V.M. Goldschmidt, *J. Chem. Soc.* **0**, 655 (1937)
6. A.W. Hofmann, *Nature* **385**, 218 (1997)
7. P.R. Kyle, D. Seward, *Geology* **12**, 487 (1984)

8. S.L. de Silva, P.W. Francis, J. Volcanol. Geoth. Res. **37**, 133 (1989)
9. P. Shane, I. Smith, New Zeal. J. Geol. Geop. **43**, 569 (2000)
10. S.L. Donoghue, J. Vallance, I.E.M. Smith, R.B. Stewart, J. Quat. Sci. **22**, 395 (2007)
11. E.L. Tomlinson, T. Thordarson, W. Müller, M. Thirlwall, M.A. Menzies, Chem. Geol. **279**, 73 (2010)
12. J. Pearce, Episodes **19**, 120 (1996)
13. J.-H. Yu, X. Xu, S.Y. O'Reilly, W.L. Griffin, M. Zhang, Lithos **67**, 77 (2003)
14. J.W. Goodge, P. Myrow, I.S. Williams, S.A. Bowring, J. Geol. **110**, 393 (2002)
15. B. Schmickler, D.E. Jacob, S.F. Foley, Lithos **75**, 173 (2004)
16. J.J. Gurney, P. Zweistra, J. Geochem. Explor. **53**, 293 (1995)
17. C. Dupuis, G. Beaudoin, Miner. Dep. **46**, 319 (2011)
18. R.J. Parker, K. Nicholson, in Proceedings of the 12th New Zealand Geothermal Workshop, Auckland University, Auckland, 1990
19. J.D. Grigsby, J. Sediment. Res. **62**, 331 (1992)
20. P.R. Duller, J.D. Floyd, Geol. Mag. **132**, 557 (1995)
21. E. Martínez-Monasterio, R.W. Duck, W.E. Stephens, J. Walden, Scot. J. Geol. **42**, 137 (2006)
22. R.S. Harmon, K.M. Shughrue, J.J. Remus, M.A. Wise, L.J. East, R.R. Hark, Anal. Bioanal. Chem. **400**, 3377 (2011)
23. R.R. Hark, J.J. Remus, L.J. East, R.S. Harmon, M.A. Wise, B.M. Tansi, K.M. Shughrue, K.S. Dunsin, C. Liu, Spectrochim. Acta Part B **74–75**, 131 (2012)
24. A.I. Fridman, J. Geochem. Explor. **38**, 1 (1990)
25. M.I. Leybourne, E.M. Cameron, Geochem-Explor. Env. A. **10**, 99 (2010)
26. A. Marie, A. Vengosh, Ground Water **39**, 240 (2001)
27. S. Helgen, A. Davis, A. Nicholson, Environ. Forensics **4**, 255 (2003)
28. M.G. Lawrence, A. Greig, K.D. Collerson, B.S. Kamber, Appl. Geochem. **21**, 839 (2006)
29. C. Reimann, M. Birke, *Geochemistry of European Bottled Water* (Borntraeger Verlagbuchhandlung, Stuttgart, 2010)
30. D.E. Walling, P.N. Owens, G.J.L. Leeks, Hydrol. Process. **13**, 955 (1999)
31. G.F. Birch, Int. J. Environ. Pollut. **13**, 573 (2000)
32. E. de Miguel, S. Charlesworth, A. Ordóñez, E. Seijas, Sci. Total Environ. **340**, 137 (2005)
33. J. Liu, Y. Saito, X. Kong, H. Wang, L. Zhao, Cont. Shelf Res. **29**, 846 (2009)
34. A.L. Collins, Y. Zhang, D.E. Walling, S.E. Grenfell, P. Smith, Sci. Total Environ. **408**, 5461 (2010)
35. D.R. Muhs, C.A. Bush, K.C. Stewart, T.R. Rowland, R.C. Crittenden, Quat. Res. **33**, 157 (1990)
36. B. Bousquet, G. Travaillé, A. Ismaël, L. Canioni, K.M.-L. Pierrès, E. Brasseur, S. Roy, I.I. Hecho, M. Larregieu, S. Tellier, M. Potin-Gautier, T. Boriachon, P. Wazen, A. Diard, S. Belbèze, Spectrochim. Acta Part B **63**, 1085 (2008)
37. T.L. Potter, in *Petroleum Contaminated Soils*, vol. 3, ed. by P.T. Kostecki, E.J. Calabrese (Lewis Publishers Inc., 1990), pp. 83–92
38. I.R. Kaplan, Y. Galperin, S.-T. Lu, R.-P. Lee, Org. Geochem. **27**, 289 (1997)
39. R.L. Kaufman, H. Dashti, C.S. Kabir, J.M. Pederson, M.S. Moon, R. Quttainah, H. Al-Wael, SPE Reserv. Eval. Eng. **5**, 190 (2002)
40. I. Eide, K. Zahlsen, Energ. Fuel. **19**, 964 (2005)
41. C.A. Redmount, M.E. Morgenstein, J. Archaeol. Sci. **23**, 741 (1996)
42. K.H. Wedepohl, Glass Sci. Tech. **70**, 246 (1997)
43. M. Markham, P.A. Floyd, Proc. Ussher **9**, 218 (1998)
44. J.D. Greenough, M.P. Gorton, L.M. Mallory-Greenough, Geoarchaeol. **16**, 763 (2001)
45. M.D. Glascock, Acc. Chem. Res. **35**, 611 (2002)
46. L.M. Mallory-Greenough, J. Baker, J.D. Greenough, Can. J. Archaeol. **26** (2002)
47. A. Adriaens, Spectrochim. Acta B **60**, 1503 (2005)
48. R.H. Tykot, Acc. Chem. Res. **35**, 618 (2002)
49. A. Abduriyim, H. Kitawaki, Gems Gemol. **42**, 98 (2006)

50. C.E. McManus, N.J. McMillan, R.S. Harmon, R.C. Whitmore, F.C. DeLucia, A.W. Miziolek, *Appl. Opt.* **47**, 72 (2008)
51. B. Giussani, D. Monticelli, L. Rampazzi, *Anal. Chim. Acta* **635**, 6 (2009)
52. G.R. Rossman, *Elements* **5**, 159 (2009)
53. D.C. Alvey, K. Morton, R.S. Harmon, J.L. Gottfried, J.J. Remus, L.M. Collins, M.A. Wise, *Appl. Opt.* **49**, C168 (2010)
54. J.J. Remus, R.S. Harmon, R.R. Hark, G. Haverstock, D. Baron, I.K. Potter, S.K. Bristol, L.J. East, *Appl. Opt.* **51**, B65 (2012)
55. G. Rapp, *Annu. Rev. Earth Planet. Sci.* **15**, 97 (1987)
56. R.S. Harmon, R.E. Russo, R.R. Hark, *Spectrochim. Acta A* (**in press**) (2013)
57. B. Naes, S. Umpierrez, S. Ryland, C. Barnett, J. Almirall, *Spectrochim. Acta A* **63**, 1145 (2008)
58. M.S. Shackley, *Obsidian: Geology and Archeology in the North American Southwest* (The University of Arizona Press, 2005)
59. R.C. Wiens, S. Maurice, *Geol. Soc. Am. Abs. Prog.* **44**, 190 (2012)
60. R.S. Harmon, J.J. Remus, J. Gottfried, J. Gonzalez, D. Wong, D. Baron, The effects of LIBS laser wavelength on the identification of obsidian artifact provenance. Paper presented at the LIBS 2010, 6th international conference on laser-induced breakdown spectroscopy, Memphis, TN, September 13–17, 2010
61. A. Hrdlička, L. Prokeš, M. Galiová, K. Novotný, A. Vitešnicková, T. Helešicová, V. Kanický, *Chem. Pap.* **67**, 546 (2013)
62. J.L. Gottfried, R.S. Harmon, F.C. De Lucia Jr, A.W. Miziolek, *Spectrochim. Acta B* **64**, 1009 (2009)
63. R.T. Wainner, R.S. Harmon, A.W. Miziolek, K.L. McNesby, P.D. French, *Spectrochim. Acta, Part B* **56**, 777 (2001)
64. M.Z. Martin, S.D. Wullschleger, C.T. Garten, A.V. Palumbo, *Appl. Opt.* **42**, 2072 (2003)
65. C. Fabre, M.-C. Boiron, J. Dubessy, A. Moissette, *J. Anal. At. Spectrom.* **14**, 913 (1999)
66. D.W. Hahn, W.L. Flower, K.R. Hencken, *Appl. Spectrosc.* **51**, 1836 (1997)
67. T. Kim, C.T. Lin, Y. Yoon, *J. Phys. Chem. B.* **102**, 4284 (1998)
68. K. Novotný, J. Kaiser, M. Galiová, V. Konečná, J. Novotný, R. Maliona, M. Liška, V. Kanický, V. Otruba, *Spectrochim. Acta, Part B* **63**, 1139 (2008)
69. V. Zorba, X. Mao, R.E. Russo, *Spectrochim. Acta, Part B* **66**, 189 (2011)
70. T. Čtvrtníková, F.J. Fortes, L.M. Cabalin, J.J. Laserna, *Appl. Spectrosc.* **61**, 719 (2007)
71. T. Čtvrtníková, F.J. Fortes, L.M. Cabalin, V. Kanický, J.J. Laserna, *Surf. Interface Anal.* **41**, 714 (2009)
72. S.K. Sharma, A.K. Misra, P.G. Lucey, R.C. Weins, S.M. Clegg, *Spectrochim. Acta, Part B* **68**, 1036 (2007)
73. F. Hilbk-Kortenbruck, R. Noll, P. Wintjens, H. Falk, C. Becker, *Spectrochim. Acta, Part B* **56**, 933 (2001)
74. S.L. Lui, Y. Godwal, M.T. Taschuk, Y.Y. Tsui, R. Fedosejevs, *Anal. Chem.* **80**, 1995 (2008)
75. S.K. Sharma, A.K. Misra, P.G. Lucey, R.C.G. Lentz, *Spectrochim. Acta, Part A* **73**, 468 (2009)
76. N.J. McMillan, C.E. McManus, R.S. Harmon, F.C. DeLucia, A.W. Miziolek, *Anal. Bioanal. Chem.* **385**, 263 (2006)
77. R.S. Harmon, F.C. DeLucia, A.W. Miziolek, K.L. McNesby, R.A. Walters, P.D. French, *Geochem.-Explor. Env. A.* **5**, 21 (2005)
78. A.P.M. Michel, M. Lawrence-Snyder, S.M. Angel, A.D. Chave, *Appl. Opt.* **46**, 2507 (2007)
79. A.S. Eppler, D.A. Cremers, D.D. Hickmott, A.C. Koskelo, *Appl. Spectrosc.* **50**, 1175 (1996)
80. S.I. Gornushkin, I.B. Gornushkin, J.M. Anzano, B.W. Smith, J.D. Winefordner, *Appl. Spectrosc.* **56**, 433 (2002)
81. P. Yaroshchuk, D.L. Death, S.J. Spencer, *Appl. Spectrosc.* **264**, 1335 (2010)
82. A. Ciucci, M. Corsi, V. Palleschi, S. Ratelli, A. Slavetti, E. Tognoni, *Appl. Spectrosc.* **53**, 960 (1999)

83. E. Tognoni, G. Cristoforetti, S. Legnaiolia, V. Palleschi, *Spectrochim. Acta, Part B* **65**, 1 (2010)
84. I. Borgia, L.M.F. Burgio, M. Corsi, R. Fantoni, V. Palleschi, A. Salvetti, M.C. Squarcialupi, E. Tognoni, *J. Cult. Herit.* **1**, S281 (2000)
85. D. Bilajic, M. Corsi, G. Cristoforetti, S. Lehnaioli, V. Palleschi, A. Salvetti, E. Tognoni, *Spectrochim. Acta, Part B* **57**, 339 (2002)
86. F.C. DeLucia Jr, J.L. Gottfried, *Mater. Today* **14**, 274 (2011)
87. R. Wisbrun, I. Schechter, R. Neissner, H. Schroder, K.L. Kompa, *Anal. Chem.* **66**, 2964 (1994)
88. J.O. Cáceres, J.T. López, H.H. Telle, A.G. Ureña, *Spectrochim. Acta, Part B* **56**, 831 (2001)
89. R.S. Harmon, J.J. Remus, C. McManus, F.C. DeLucia, J. Gottfried, A.W. Miziolek, *Appl. Geochem.* **24**, 1125 (2009)
90. J.M. Andrade-Garda, *Basic Chemometric Techniques in Atomic Spectroscopy* (Royal Society of Chemistry, Cambridge, 2009)
91. M.Z. Martin, N. Labbé, N. André, S.D. Wullschleger, R.D. Harris, M.H. Ebinger, *Soil Sci. Soc. Am. J.* **74**, 87 (2009)
92. V. Motto-Ros, A.S. Koujelev, G.R. Osinski, A.E. Dudelzak, *J. Europ. Opt. Soc. Rap. Public.* **3**, 08011 (2008)
93. E.C. Ferreira, D.M.B.P. Milori, E.J. Ferreira, R.M. DaSilva, L. Martin-Neto, *Spectrochim. Acta A* **63**, 1216 (2008)
94. J.-B. Sirven, B. Bousquet, L. Canioni, L. Sarger, *Anal. Chem.* **78**, 1462 (2006)
95. N.J. McMillan, C. Montoya, W.H. Chesner, *Appl. Opt.* **51**, B213 (2012)
96. J.-B. Sirven, B. Sallé, P. Mauchien, J.-L. Lacour, S. Maurice, G. Manhes, *J. Anal. At. Spectrom.* **22**, 1471 (2007)
97. J. Remus, K.S. Dunsin, *Appl. Opt.* **51**, B49 (2012)
98. J.J. Remus, J.L. Gottfried, R.S. Harmon, A. Draucker, D. Baron, R. Yohe, *Appl. Opt.* **49**, 120 (2010)
99. R.S. Harmon, F.C. DeLucia, C.E. McManus, N.J. McMillan, T.F. Jenkins, M.E. Walsh, A.W. Miziolek, *Appl. Geochem.* **21**, 730 (2006)
100. N.J. McMillan, R.S. Harmon, F.C. DeLucia, A.W. Miziolek, *Spectrochim. Acta, Part B* **62**, 1528 (2007)
101. T.G.G. Laboratory, *Jewellery News Asia*, 66 (2006)
102. R.W. Hughes, *Austral. Gemmol.* **19**, 52 (1995)
103. M. Guillion, D. Günther, *Spectrochim. Acta A* **56**, 1219 (2001)
104. H.A. Hänni, M.S. Krzemnicki, K. L., J.P. Chalain, *Z. Dtsch. Gem. Gesell.* **53**, 79 (2004)
105. M.S. Krzemnicki, H.A. Hänni, R. Walters, *Gems Gemol.* **40**, 314 (2004)
106. D.B. Hoover, B. Williams, *Austral. Gemmol.* **23**, 146 (2007)
107. J. Gottfried, R.S. Harmon, R.R. Hark, F.C. De Lucia Jr, A.W. Miziolek, Analysis and discrimination of volcanic rocks by benchtop and standoff LIBS. Paper presented at the Joint Meeting of The Geological Society of America, Soil Science Society of America, American Society of Agronomy, Crop Science Society of America, Gulf Coast Association of Geological Societies with the Gulf Coast Section of SEPM, Houston, TX
108. S.K. Bristol, R.R. Hark, R.S. Harmon, J.J. Remus, L.J. East, Analysis of historical rocks using laser-induced breakdown spectroscopy (LIBS). Paper presented at the 241st American Chemical Society National Meeting & Exposition, Anaheim, CA, 27–31 March 2011
109. L. Haarklau, L. Johnson, D.L. Wagner, *Fingerprints in the Great Basin: The Nellis Air Force Base Regional Obsidian Sourcing Study* (U.S. Army Corps of Engineers, Fort Worth District, 2005)
110. R.S. Harmon, J.J. Remus, S.K. Bristol, I.K. Potter, R.R. Hark, L.J. East, Connecting obsidian artifacts with their sources using laser-induced breakdown spectroscopy (LIBS). Paper presented at the 38th Annual Meeting of the Federation of Analytical Chemistry and Spectroscopy Societies (FACSS), Reno, NV
111. F. Melcher, M.A. Sitnikova, T. Graupner, N. Martin, T. Oberthür, F. Henjes-Kunst, E. Gäbler, A. Gerdes, H. Brätz, D.W. Davis, S. Dewaele, *SGA News* **23**, 6 (2008)

112. C. Savu-Krohn, G. Rantitsch, P. Auer, F. Melcher, T. Graupner, *Nat. Resour. Res.* **20**, 177 (2011)
113. H.-E. Gäbler, F. Melcher, T. Graupner, A. Bahr, M.A. Sitnikova, F. Henjes-Kunst, T. Oberthür, H. Brätz, A. Gerdes, *Geostan. Geolanal. Res.* **35**, 431 (2011)
114. K.M. Shughrue, K.S. Dunsin, M.A. Wise, J.J. Remus, L.J. East, J. Gonzalez, R.R. Hark, R.S. Harmon, LIBS analysis of columbite-tantalite: A real-time technique for the analysis of conflict minerals in the field? Paper presented at the 3rd North American Symposium on Laser-induced Breakdown Spectroscopy, Clearwater Beach, FL, 18–20 July 2011
115. B.M. Tansi, R.R. Hark, L.J. East, J.J. Remus, R.S. Harmon, M.A. Wise, Laser-induced breakdown spectroscopy (LIBS) for geochemical fingerprinting of columbite-tantalite sources. Paper presented at the 243rd American Chemical Society National Meeting & Exposition, San Diego, CA, 25–29 March 2012
116. IndexMundi, Tin Monthly Price—US Dollars per Metric Ton. <http://www.indexmundi.com/commodities/?commodity=tin&months=360>. Accessed 20 May 2013
117. I.K. Potter, B.M. Tansi, K. Hilferding, R.R. Hark, J.J. Remus, M.A. Wise, R.S. Harmon, L.J. East, Determination of source location of the “conflict mineral” cassiterite using laser-induced breakdown spectroscopy (LIBS). Paper presented at the 243rd American Chemical Society National Meeting & Exposition, San Diego, CA, 25–29 March 2012
118. C.H. Aurand, *Chem. Eng. News* **90**, 36 (2012)
119. H.-E. Gabler, S. Rehder, A. Bahr, F. Melcher, S. Goldmann, *J. Anal. Atomic Spectrom* (2013)
120. . M.J.C. Pontes, J. Cortez, R.K.H. Galvão, C. Pasquini, M.C.U. Araújo, R.M. Coelho, M.K. Chiba, M.F.d. Abreu, B.E. Madari, *Anal. Chim. Acta* **642**, 12 (2009)
121. S. Jantzi, J.R. Almirall, *Anal. Bioanal. Chem.* **400**, 3341 (2011)
122. M. Gaft, E. Dvir, H. Modiano, U. Schone, *Spectrochim. Acta, Part B* **63**, 1177 (2008)
123. W. Yin, L. Zhang, L. Dong, W. Ma, S. Jia, *Appl. Spectrosc.* **63**, 865 (2009)